Biomedical Signal Processing and Control 39 (2018) 237–262

Contents lists available at ScienceDirect

Biomedical Signal Processing and Control

journal homepage: www.elsevier.com/locate/bspc

Review Article

Techniques and algorithms for computer aided diagnosis of pigmented skin lesions—A review

Sameena Pathan[a,*], K. Gopalakrishna Prabhu[b], P.C. Siddalingaswamy[a]

[a] Department of Computer Science and Engineering, Manipal Institute of Technology, Manipal University, Manipal, India
[b] Department of Biomedical Engineering, Manipal Institute of Technology, Manipal University, Manipal, India

ARTICLE INFO

Article history:
Received 16 October 2016
Received in revised form 19 June 2017
Accepted 20 July 2017
Available online 30 August 2017

Keywords:
Acquisition
Classification
Dermoscopy
Melanoma
Pigmented skin lesions (PSLs)
Segmentation

ABSTRACT

Computerized image analysis methods for dermoscopy are primarily of great interest and benefit, as it provides significant information about the lesion, which can be of pertinence for the clinicians and a stand-alone warning implement. Computer-based diagnostic systems require dedicated image processing algorithms to provide mathematical descriptions of the suspected regions, such systems hold a great potential in oncology. In this paper, we have performed a review of the state of art techniques used in computer-aided diagnostic systems, by giving the domain aspects of melanoma followed by the prominent techniques used in each of the steps. The steps include dermoscopic image pre-processing, segmentation, extraction and selection of peculiar features, and relegation of skin lesions. The paper also presents cognizance to judge the consequentiality of every methodology utilized in the literature, in addition to the corresponding results obtained in this perspective. The inadequacies and the future research directions are accentuated.

© 2017 Elsevier Ltd. All rights reserved.

Contents

* Corresponding author.
E-mail addresses: sameena.pathan.k@gmail.com (S. Pathan), gk.prabhu@manipal.edu (K.G. Prabhu), pcs.swamy@manipal.edu (P.C. Siddalingaswamy).

http://dx.doi.org/10.1016/j.bspc.2017.07.010
1746-8094/© 2017 Elsevier Ltd. All rights reserved.

1. Introduction

Large scale systematic research and advancement of computer availed diagnosis system began in 1980s, although early attempts prevailed from 1960s. Owing to the fast pace in growth of computer vision techniques for analyzing medical imaging data, significant research is carried on to provide better diagnosis and prediction of diseases. Skin cancer is the unconstrained magnification of anomalous skin cells. Skin cancer is the most frequent type of cancer and can be highly truculent. Unrepaired DNA or genetic faults cause skin cell mutations, consequently causing the skin cells to proliferate rapidly, forming malignant tumors. One out of every five Americans will probably foster skin cancer in their lifetime according to skin cancer foundation. White skinned people are commonly afflicted by malignant melanoma due to cumbersomely heavy sun exposure [1]. In 2016, an estimated 76,380 incipient cases of melanoma was predicted to be diagnosed [2,3]. Melanoma accounts for only 1% of all skin cancer cases, but astronomical mass number of skin cancer deaths [1–4]. Prognosis of melanoma patients is inversely proportional to the tumor thickness. As the tumor thickness increases, the survival rate decreases. Melanoma is detectable by simple observation, since it is confined to the skin. However, it is further liable to metastasize and spread to lymph nodes thus incrementing the caliber of malignancy.

Primitive diagnosis of melanoma rely primarily upon patient vigilance and precise assessment by a medical practitioner. There subsists more immensely colossal diagnostic variations in additament to deficient knowledge of the test methods. Dermoscopy is an in vivo evaluation method for the structures within the epidermis and dermis. It is an essential implement for dermatologists and plastic surgeons, endeavoring early diagnosis of skin cognate disorders [5]. It is additionally known as epiluminoscopy and epiluminiscent microscopy. Higher magnification and visualization of subsurface structures and patterns are the major requisites of dermoscopy [6]. Digital dermoscopy images can be analyzed for distinguishing features by medical expert perspective or by machine perspicacity [7]. Astronomically, immense number of minor caliber features are extracted and analyzed by computer availed diagnostic systems from the dermoscopic images. It apperceives features through mathematical and statistical analysis of dermoscopic images thus enabling detection of features that cannot be perceived by human ocular perceivers. Numerous low-level features are extorted based on the categorization strategy from the Region of Interest (ROI) and relegated accordingly as malignant melanoma and benign PSL, which consequently amends the diagnostic precision over even well trained and experienced clinicians [8,9]. Significant endeavor has been made to intensify the clinical interpretation of melanoma in the recent years, owing to the exigency and paramountcy of early and precise diagnosis. Image pre-processing, segmentation of the lesions from the background, extraction of dermoscopic features specific to melanoma and classification form the major design issues for opportune skin lesions depiction.

In 2016, the ISBI challenge on “Skin Lesion Analysis towards Melanoma Detection” was hosted by ISIC. The challenge aimed to support research and development of algorithms for automated analysis of melanoma [10]. The challenge was sub-divided into three tasks: Segmentation of the lesion, dermoscopic feature detection and classification of lesions as benign and malignant. The second and third tasks were further sub-divided into sub tasks. The training and test dataset consisted of 900 and 379 images respectively. The lesion segmentation task (I) involved automated localization of lesion areas in the form of binary masks. The dermoscopic feature detection involved two sub tasks namely, dermoscopic feature classification (II) and dermoscopic feature segmentation (IIB). The former involved the detection of two clinically defined features: globules and streaks. The latter involved the indication of dermoscopic features in the form of binary masks. The third task was also divided into two sub tasks: classification of lesion as malignant or benign based on the original image, formed the first sub task (III) and classification of lesion as malignant or benign based on the segmented masks, formed the second sub task (IIIB). The highest performance accuracies obtained for each of the tasks are 0.953, 0.916, 0.916, 0.855 and 0.855 for part I, II, IIB, III, IIIB respectively. The outcome of the challenges that were observed are as follows.

1. Promising results were obtained from the perspective of dermoscopic feature extraction. However, there exists a scope for further development.
2. The performance of the algorithms in terms of disease recognition is within the range as provided by expert dermatologist.

Although, the ISIC challenge has been concluded the image datasets are available for further research and development. The lesion images are annotated with pathological diagnosis information, lesion level attributes, and sub-lesion level features. December 10, 2016 marked the commencement of the 2017 ISBI challenge on “Skin Lesion Analysis towards Melanoma Detection” hosted by ISIC [11]. The American Cancer Society has estimated 87,110 melanoma

cases for the year 2017 [12]. The challenge differs slightly from the 2016 ISBI challenge in terms of a larger image dataset, validation dataset, dermoscopic features for extraction (network, negative network, streaks, and Milla-like cysts), classification categories (Melanoma, Nevus, and Seborrheic keratosis) and new evaluation metrics. The challenge provides 2000 images for training data, 150 images as validation dataset, and 600 images as test dataset. The images have been annotated by recognized melanoma experts and a subset of these images include dermoscopic feature markups.

This paper presents a cumulated overview of steps utilized by the subsisting systems, for developing an automatic diagnostic system for pigmented skin lesion detection and relegation. It highlights the design features and analysis procedures from medical as well as engineering perspective, thus availing researchers with the cognizance of felicitous techniques that eventually lead to the refinement of the current approaches for reducing melanoma mortality rate.

The organization of the review paper is as follows. Section 2 gives the background of the skin cancer. Section 3 highlights the image acquisition techniques used by clinicians. Sections 4 and 5 present the pre-requisite methodologies of image preprocessing and segmentation. Section 6 gives feature extraction followed by feature selection in the Section 7. Classification and Performance evaluation are given in Sections 8 and 9. The paper concludes with the discussion regarding the state of art methodologies highlighting the research gaps in Section 10.

2. Skin cancer

The most astronomically immense organ of the human body is the skin, a highly organized structure consisting of epidermis, dermis and hypodermis. Auspice, sensation and thermoregulation are the three main functions of the skin. The skin provides an excellent aegis from aggression of the environment. Stratum corneum, the top layer of the epidermis, is optically neutral protective layer with varying thickness. The stratum corneum consists of keratinocytes that engender keratin responsible for availing the skin to forefend the body. The incidence of light on the skin is scattered due to stratum corneum. The epidermis contains melanocytes in its basal layer. Melanocytes engender the skin pigment termed as melanin, which provides the tan or brown color of the skin. Melanocytes act as a filter and bulwark the skin from deleterious Ultraviolet (UV) sun rays by incrementing the engenderment of melanin. The extent of absorption of UV rays depends on concentration of melanocytes. The middle layer of the skin is the dermis consisting of collagen fibers, sensors, receptors, blood vessels and nerve ends. It gives elasticity and vigor to the skin [13].

Deoxyribonucleic Acid (DNA) is composed of molecules called nucleotides. Nucleotide comprises of a phosphate and a sugar group along with a nitrogen base. Nitrogen bases are four types namely Adenine (A), Thymine (T), Guanine (G) and Cytosine (C). Nitrogen bases order in the DNA sequence forms genes. Genes are responsible for the formation, multiplication, division and death of the cells. Oncogenes are responsible for multiplication and division of cells. Protective genes are known as tumor suppressor genes. Customarily, they inhibit cell growth by monitoring how expeditiously cells divide into incipient cells, rehabilitating mismatched DNA, and controlling when a cell dies. The uncontrollable growth of cells is due to the mutations of the tumor suppressor gene eventually forming a mass called a tumor (cancer). Ultra violet rays can damage the DNA, consequently this damage causes the melanocytes to produce melanin at a highly abnormal rate. Although, certain amount of UV rays must enter the skin to provide vitamin D, excess causes PSLs [14]. The malignant tumor due to abnormal growth of melanocytes is known as melanoma [15].

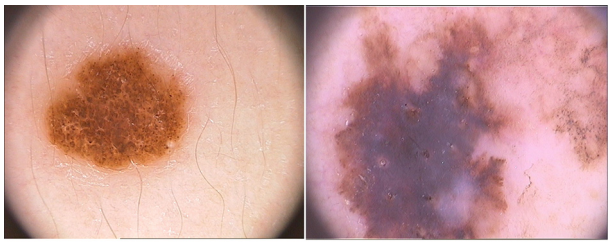

Fig. 1. Morphology of PSL (a) Benign skin lesion (b) Malignant skin lesion [41].

Melanomas often start as minuscule, mole-like with a gradual change in size and color variation. The color of melanin essentially depends on its localization in the skin. The color ebony is due to melanin location in the stratum corneum and the upper epidermis, light to dark brown, gray to gray-blue and steel-blue are observed in the upper epidermis, papillary dermis and in the reticular dermis respectively. In case of benign lesions, the exorbitant melanin deposit is present in the epidermis. Melanin presence in the dermis is the most consequential designation of melanoma causing prominent vicissitude in skin coloration. There are several other designations for melanoma, which includes thickened collagen fibers in addition to pale lesion areas with a large blood supply at the periphery. The gross morphologic features additionally includes shape, size, coloration, border and symmetry of the pigmented lesion. Biopsy and histology [16], are required to perform explicit diagnosis in case the ocular approximation corroborates a suspicion of skin cancer. The Fig. 1 illustrates the morphology of PSLs. According to microscopic characterizations of the lesion, there are four major categories of melanoma namely Superficial Spreading Melanoma (SSM), Nodular Melanoma (NM), Lentigo Malignant Melanoma (LMM), and Acral Lentiginous melanoma (ALM).

3. Imaging modalities and image acquisition

Symptoms such as blood oozing, itching and suppuration were considered in earlier prediction of melanoma. Unaided visual inspection is suboptimal and does not provide enough information for a precise early diagnosis of skin cancer. Subtle features require further magnification to be visualized limpidly by adept observers to detect and interpret many morphological features [17]. Morphological evolutionary vicissitudes in a mole with deference to size and color can be regarded as preliminary stages of melanoma. Melanin presence in the dermis is the most consequential denotement of melanoma. However, due to homogeneous possession of melanin characteristics by insitu and benign nevi, it cannot be regarded as an exclusive diagnosis paradigm. Friedman et al. [18], introduced the asymmetry, border, color and diameter rule (ABCD) that sanctioned primitive detection of large figures of melanomas. Morphological vicissitudes in lesion over a period was included as fifth criterion.

3.1. Imaging modalities

Numerous imaging modalities were developed to avail dermatologist to overcome problems associated with apperception of minuscule sized melanomas, ascertaining correct in vivo diagnosis of benign melanocytic nevi from melanoma.

Kolhaus was the first one to start skin surface microscopy in 1663 to study minuscule vessels in nail folds [19]. Johann Saphier a German dermatologist coined the term dermatoscopy in 1920 and thereafter employed this proficiency for PSL evaluation [20]. Distinctive diagnosis of PSL as benign and malignant utilizing surface microscopy was observed by Rona Mackie [21]. Dermoscopy

additionally kenned as epiluminescence microscopy (ELM) is a non-invasive method that sanctions in vivo evaluation of colors and microstructure of the epidermis. The dermo-epidermal junction and the papillary dermis are not visible to unclad ocular technique [22]. These structures form the histopathological features to determine the level of malignancy, further designating whether the lesion ought to be biopsied [23]. The fundamental principle of dermoscopy, is transillumination of the lesion. Stratum corneum, the top most layer of the skin is optically neutral. Due to the incidence of visible radiation on the surface of the skin, reflection occurs at the stratum corneum air interface because of vicissitude in index of refraction (air n = 1, refraction of stratum corneum is n = 1.45) [24]. Linkage fluids applied on the surface of the skin provide higher magnification and access to deeper layers of the skin structures, since oily skin sanctions light to pass through it [25]. Despite its cognizance of essential angles, for example, best submersion liquid to utilize, the scope of observable structures is circumscribed in comparison to other techniques providing a potentially subjective diagnostic precision. It was demonstrated that the diagnostic precision is dependent on the dermatologist experience [26]. Dermoscopy was used by majority of physicians in order to reduce patient concern and provide early disclosure as per the overview. Dermatologist's perception designated traditional methods to be more efficacious compared to dermoscopy [23,27].

In vivo confocal laser scanning microscopy (CLSM) is a novel imaging implement that sanctions the investigation of skin morphology in legitimate period at a resolution equipollent to that of conventional microscopes [28]. In CSLM, a focused laser beam is utilized to enlighten a solid point inside the skin and the reflection of light starting there is measured. Gray-scale image is built by examining the territory parallel to the skin surface. Sundry profundities can furthermore be imaged to form optical areas. Sidelong resolutions can be utilized to induce the pictures [29]. The epidermis, papillary dermis, and upper reticular dermis can be outwardly seen at resolutions commensurable to histology. A sensitivity of 88% and specificity of 71% was acquired utilizing CSLM according to the review published in 2012 [30]. Cost up to $50,000 to $100,000 are associated with confocal magnifying lens which represents a noteworthy disadvantage in utilizing CSLM [30].

Optical Coherence Tomography (OCT) is a high-determination non-obtrusive imaging that has as of late been presented in restorative examinations. The sensitivity and specificity varies between 79% to 94% and 85% to 96% respectively [31]. The diagnosis utilizing OCT is less precise compared to clinical diagnosis. However, a higher precision was obtained for distinguishing lesions from normal skin.

Spectrophotometric or spectral analysis of skin lesions refers to the utilization of a skin imaging contrivance [32]. The SIA scope avails in the diagnosis of lesions as diminutive as 2 mm. In particular, it can increment the performance of practicing clinicians in the early diagnosis of the deadly disease. A large study showed that SIA scope had the same sensitivity and specificity as to dermatoscopy performed by skillful dermatologist and hence, it did not provide sufficient advantage in diagnosing melanoma [5]. Apart from these, the utilization of photographic equipment's that provide Total Body Photography [33] representing the patient entire cutaneous surface is also been utilized. However, it proves to be sumptuous and time consuming. Melafind can engender multispectral sequence of images in less than three seconds [34]. The interpretation of these images gets arduous due to the involution of the optical processes involved. Ultrasound imaging [35] and Magnetic Resonance Imaging (MRI) [36] provide information regarding patterns associated with lymph nodes and depth extent of the underlying tissue respectively, thus assisting in tenacity of melanoma stages. Additionally, a few other imaging modalities include MoleMax, MoleAnalyzer, Real time Raman spectroscopy, Electrical impedance spectroscopy, Fiber diffraction, Thermal imaging. Nagaoka et al. [37], provides a review of recent diagnostic technologies for melanoma detection.

Computer-Aided Diagnostic (CAD) systems are introduced for digital dermoscopic images to provide quantitative and target assessment of the skin lesion to help clinicians in demonstrative and prognostic undertakings. Due to the inter and intra-observer variabilities determination of melanoma is innately subjective. The exactness related in diagnosing melanoma is assessed to be 75% to 84% [38]. Thus, a computer-aided second opinion expands the precision of analysis along these lines diminishing the quantity of superfluous biopsies. In the first phase, the dermoscopic image needs to be pre-processed to eliminate the artifacts like hair, noise, air bubbles etc., it is followed by disseverment of the lesion from the background skin, in order to extract and select relevant geometrical and texture features required for differentiating malignant melanoma from benign nevi. To set benchmarks for diagnostic system development efficient and computationally more expeditious image processing algorithms are required. Researchers at Stanford University, have developed an automated diagnostic tool for identification of skin lesions. The study involved a deep learning algorithm built on the Google Net Inception V3 architecture, trained using 1.28 million images [39]. However, according to the opinion of the dermatologist and researchers at Oregon Health & Science University, the Stanford program needs to be tested for tougher cases before accepting it in a clinical setting [40]. In order to accept a CAD tool in clinical setting, the CAD tool needs to provide the dermatologist with the grounds of clinical decision.

3.2. Publicly available databases

To develop a reliable and a robust CAD system for melanoma detection, it is crucial to have a diverse image dataset. An overview of the publicly available dermatological databases and atlases is given in Table 1. Details such as, total number of images, annotation information from the perspective of dermoscopic features and lesion type are also been highlighted.

The above mentioned databases can be used by researchers to develop algorithms for detection of the pigmented skin lesions. Dermquest and Dermis datasets can be downloaded freely from Image and Vision Processing Lab, University of Waterloo [49]. Joint Photographic Experts Group (JPEG) images are compressed image formats, with limited amount of details. Thus JPEG dermoscopic images may not be suitable for skin lesion analysis since such images would limit the CAD capabilities.

4. Image pre-processing

Detection of lesion is a crucial and challenging task in dermatoscopic images due to several facts. The move between the lesion and the circumventing skin is smooth, the images acquired from digital cameras are hindered by shadows that seem related in shading as the skin lesion. Artifacts such as air bubbles, hair, ebony frames, ink markings, uneven illumination and noise shape a portion of dermoscopic pictures. These artifacts perplex the further processes of border detection and feature extraction. Everything that might alter and corrupt the image, consequently obstructing the process of developing an efficient CAD system for melanoma diagnosis, needs to be localized and abstracted or superseded. To facilitate border detection process many approaches have been applied that include masking, image resizing, filtering, color space conversions, hair detection and removal, reduction of noise and artifacts complicating the process bringing about loss of exactness and expansion in computational time.

Single channel (scalar) or multichannel (vector) images of the skin lesions may be used for pre-processing. The blue channel of the

Table 1
Overview of the Publicly Available databases.

Database	No. of Images	No. of Lesion Images	Dermoscopic and Lesion feature Annotation	Ref
ISIC Archive (2016 ISBI challenge)	900	273- Melanoma 627- Non-Melanoma	Globules Streaks	[10]
ISIC Archive (2017 ISBI challenge)	2000	374- Melanoma 254- Seborrheic keratosis 1372- Benign Nevi	Network Negative Network Milla-like cysts Streaks	[11]
pH 2	200	80- Common Nevi 40- Melanomas 80- Atypical nevi	Asymmetry Colors Pigment Network Dots Globules Streaks Regression Areas Blue-White veil	[41]
Dermatology Atlas	8084	80-Melanomas	NA	[42]
Dermnet Skin Disease Atlas	23,000	190- Melanomas	NA	[43]
Danderm	3000	59- Malignant, 71- Benign	NA	[44]
EDRA Interactive Atlas of Dermoscopy[a]	NA	Invasive melanomas, In situ melanoma, Spitz nevi, Clark nevi, Bowen disease (80- Melanomas, 120-Benign)	Pigment Network Irregular Dots Globules	[45]
Dermofit Image Library[a]	1300	76-Melanomas	NA	[46]
Dermquest	NA	308- Melanoma	Type of Melanomas	[47]
Dermis	NA	300-Melanoma	NA	[48]

[a] Require fee.

RGB image is most widely used channel, as the lesions can be more predominantly visible in this channel. In few cases, the gray level image is also used for pre-processing. A few works have been conducted to change the original RGB image into a more suitable color space with the goal of improving the differentiation between the lesion and the healthy skin. Most commonly used color spaces are CIEL*a*b [50,51], CIEL*u*v [172,273] and HSV [172,200,273] color spaces. The proximate perceptual consistency of the image colors is enlarged by the use of these color spaces. The methods designed for single channel images may be used for multichannel images by applying the methods separately to individual channels and subsequently concatenating the obtained single channel results. Illumination variation in dermoscopic images negatively affects the lesion localization process, especially in macroscopic images. Recently in [52], a model for correcting illumination variation in skin lesion images based on adaptive bilateral decomposition and polynomial curve fitting was adopted. Monte-Carlo sampling method and parametric quadratic surface model is used to estimate illumination which is further used for obtaining reflectance model for illumination correction [52].

Hair pixels customarily present in the skin pictures block a portion of the sore especially boundary and lesion texture. In melanoma, apperception hair artifacts should be abstracted without altering lesion features. The directional filters were constructed by subtracting the Gaussian filter from the isotropic filter by Abuzalegah et al. [53], to recognize and discard the hair from the lesion. The gap at the region of the hair was filled with the mean of the edge pixels and stored as a pixel value at the position of the hair gap. Phantom hair builder for engendering phantom hair images that were overlaid on dermoscopic images to detect occluding hair was utilized by Wington et al. [54]. It is constructed by utilizing the HSV color space. Match filtering is applied to V channel followed by morphological thinning and Gaussian fitting to consummate the hair occlusion process. The results were compared with the images processed by dull razor software. Dull razor outperforms the method in [54], by a small amount. Dull Razor [55] performs morphological operation, bilinear interpolation and adaptive median filtering. However, essential subtle elements of the pristine images get eradicated making the lesion hazy. Morphological operations and thresholding involves generation of hair masks based on luminosity and replacing the non-masked pixels with the masked ones. It was applied to the three color components of CIEL*u*v color space [56].

Eshaver [57], is an efficacious and amended technique for hair abstraction from dermoscopic images utilizing Radon transform and filtering with Perwitt filters, it is more expeditious and can remove dark and light hair more efficaciously as compared to the subsisting and widely used Dull Razor software. Erosion and dilation using mathematical morphology is used by Michele et al. [58]. Hair is treated as long relatively straight curvilinear structure with constant width and curvature by Fleming et al. [59]. Nonetheless, this algorithm is not felicitous for crisscross hair segments and lesion images with numerous hair. PDE based automated hair removal algorithm [60], produces blur images and applies morphological closing operation with top hat operator. Image inpainting replaces gaps with color of boundaries adding texture it performs 32.7% better compared to linear interpolation [37]. However, it is not capable of reconstructing structure, and texture simultaneously. Most of these techniques results in over segmentation, undesirable blurring, and transmutations in tumor texture and color bleeding. A comparative study of hair detection and repair algorithms is presented by Abbas et al. [61], it was concluded that fast marching method achieves precise result in additament the algorithm repairs the melanoma texture.

Insufficient contrast adaptive histogram equalization for image enhancement and wiener filtering is used for image renovation [62]. Adaptive histogram equalization splits the image into rectangular regions called tiles and the contrast of these zones is upgraded by altering their nearby histograms. To enhance the contrast of dermoscopic images, optimal weights are determined to convert the RGB image to gray scale by minimizing a histogram bimodality measure [51]. Splines and second order B-splines are used for enhancement of images [64]. An unsupervised algorithm was proposed by Gomez et al. [65] for image enhancement, it evaluates an arrangement of straight mix of image groups that ultimately leads the enhancement of structures embedded in an image [65].

Another popular technique is the homomorphic filtering derived from illumination-reflectance model which require appropriate selection of frequency domain filter function [66,67]. Abbas et al. [50], performed contrast improvement by changing the power estimations of the lesion pixels utilizing color channels of CIEL*a*b space. Colors of dermoscopic images acquired with different cameras are often different as perceived by human visual system, thus proper calibration is required for establishing a relationship between device subordinate color space and a standard one. Quintana et al. addresses the color calibration problem [68]. Keeping in mind the end goal to debilitate the impact of non-uniform brightening the HSV color space was used by Ramezani et al. [154] due to the prominent visibility of the shadow effect in the V channel.

Dark frames intercede with the lesion localization technique. Celebi et al. [69], performed pixel categorization utilizing the lightness component of HSL color space by categorizing pixels below a threshold value of 20 to be termed as tenebrous. Smoothing of dermoscopic images utilizing filters abstracts artifacts from the image. Median filters [70], supersede each pixel by the median value of the neighboring pixels, it preserves some noise and details. To amend the performance of the median filters many modifications are proposed, such as recursive median filter, and weighted mean filter [71]. Adaptive recursive median filter has capability of preserving the edges [72,73]. Anisotropic filter engenders better results in image smoothing and safeguarding of edges of the skin lesions [74]. In order to eliminate the artifacts containing linear strokes, directional filters are used by tuning to a concrete orientation [75]. Directional filters have the capability to detect features in specific direction. Barata et al. [76], used directional filters predicated on 2D Gabor filters and matched filtering principle. For pre-processing of furrow like patterns, image is rotated vertically using Gaussian differentiation, and alignment is performed using histogram of directions [77].

A few works have been conducted to change the original RGB image into a more opportune color space, with the goal of improving the differentiation between the lesion and the mundane skin. All the aforementioned preprocessing undertakings are required to benefit productive division, and simply feature extraction tasks thereby prompting better demonstrative results.

5. Segmentation of skin lesions

Segmentation alludes to the dividing of an image into distinct regions containing each pixel with kindred attributes. Segmentation algorithms avail human observers to perceive the boundaries of lesions. The prosperity of image analysis depends on reliability of segmentation, but a precise partitioning of an image is generally very conundrum. Manual border detection takes into account the quandary caused by collision of tumors, wherein there is proximity of lesions of more than one type, higher caliber knowledge of lesion features are considered [78,79]. Second, the process of classification order would be less impacted by mistakes in border location. At present, there is considerable enthusiasm for the possibilities of an early screening framework predicated on the programmed investigation of dermatoscopic pictures. Segmentation ought to be an automated procedure to build up a strong stand-alone completely programmed framework for early cautioning analysis of skin lesions. In this way, a computer predicated programmed picture analyzer has an awesome potential for dermoscopy [80]. Morphological differences in appearance of skin lesions directly influence the choice of method for segmentation. The foremost reason is there subsists a relatively poor contrast between the mundane and pigmented skin lesion. Other reasons that integrate to diverse difficulties in segmentation include variations in skin tone, presence of artifacts such as hair, ink, air bubbles, ruler marks, non-uniform lighting, physical location of the lesion and most importantly lesion variations in terms of color, texture, shape, size and location in the image frame [81]. Each of these factors should be considered while designing a robust lesion segmentation algorithm. The segmentation techniques are categorized as low-level and high-level segmentation techniques to gain perspective regarding the lesion segmentation approaches. Low-level segmentation techniques are conventional approaches that include methods that are computationally simpler, faster, and require post processing. High-level segmentation techniques include those approaches that integrate low-level segmentation techniques to build sophisticated segmentation algorithms, avoid post-processing, and deal with low contrast lesion boundaries.

5.1. Low-level segmentation techniques

5.1.1. Thresholding

Pixels with values less than threshold value have been placed in one category, and the rest have been placed in the other category. Various thresholding strategies perform well. By and large, the viability of a strategy vigorously relies upon the measurable attributes of the image. Garnavi et al. [82], proposed a novel programmed segmentation algorithm utilizing color space examination and grouping based histogram thresholding, to decide the ideal channel for division of skin lesions. CIE-XYZ color space obtained from RGB is utilized [82]. An improved adaptive thresholding method is introduced by Sforza et al. [83], wherein skew estimation technique is used to facilitate correction of histogram asymmetry. The normal and the standard deviation over the brightness histogram of the entire lesion area is resolved. The strategy yields exact division of territories that are not plainly outlined reducing the number of errors in final segmentation. Comparison of thresholding algorithms [80], and review is performed in [84,85]. When the number of regions to be segmented in the image are sizably voluminous, the tenacity of optimal threshold is a tedious task. Otsu's algorithm surmounts this quandary by selecting optimal threshold [86], utilizing the discriminant criterion in order to amplify the detachability of the resultant classes [87].

5.1.2. Region based approaches

Region growing approaches exploit the paramount fact that pixels which are proximate together have homogeneous gray values. Region Growing, region merging and Mumford Shah [88], method are the most common region based methods. In Statistical Region Merging (SRM), the true region of the image are to be reconstructed by treating the image as an objective instance [89]. The Dynamic Region Merging (DRM) [90], engenders neither over merged or under merged images. The decisions are made locally and there can be a constraint for capturing the perceptual distinctions between the two neighboring local regions. Region segmentation often leads to over segmentation especially when there are diverse colors in lesion area and variations of skin texture, hence in [80], the regions are merged based on the color similarity in the CIEL*u*v color space. The simplicity and computational efficiency without the utilization of quantization or shading space transformation offered by SRM is excellent [89]. An iterative stochastic region merging based on the regional statistics is proposed in [130]. The region merging process starts from pixel level, and consequently, on a region level until convergence. Since regions are merged on pixel basis rather than region basis, the method is less prone to segmentation errors introduced due to uneven illumination and weak boundaries.

5.1.3. Edge based approaches

The Region of Interest (ROI) in dermoscopic images is generally influenced by noise levels, poor nearby complexities. Subsequently, it is unrealistic to extricate the desired regions using plenarily automatic segmentation strategies. The intensity gradient may be determined based on the magnitude of the gradient used in detecting the edge of the lesion. Some common examples of edge detectors include Canny, Sobel, Perwitt and Laplacian. Application of detectors further requires segmentation as they produce partial segmented images [91]. The results obtained by application of edge detectors to segment images is greatly influenced by noise levels, inaccuracy in detection of borders, double edge generation etc. In [92], a binary edge image of the skin lesion was created based on the fact that edges of the pigment network form cyclic graphs. Further, the binary image was converted into a graph, based on defined features in order to detect local pathological patterns of skin lesions. In [52], an iterative segmentation algorithm using canny edge detector is proposed by applying several iterations followed by median filtering of the border detected image. Canny edge detector provides low error and avoids double edges.

5.2. High-level segmentation techniques

5.2.1. Fusion based segmentation techniques

Fusion based segmentation techniques include a combination of two or more segmentation algorithms to produce a sophisticated segmentation method. Celebi et al. [78], used the thresholding strategy obtained by the combination of a group of various thresholding calculations figured inside a Markov Random Field (MRF) framework. In order to exploit the characteristics of the participating thresholding methods, and to obtain accuracies commensurable to that of the best thresholding method independently, threshold fusion was performed on blue channel by filling the matched combination yield [78]. A simple weighted Otsu thresholding method is proposed by Zortea et al. [94]. The method is adapted from Otsu threshold, initial threshold is computed by considering all the samples in the image and cross-diagonal samples weighted by an independent estimate, obtained from peripheral region skin pixels. The approach is simple and performs well for lesions occluded by coarse hair. However, poor segmentation results are obtained for images with higher variabilities at the lesion center compared to the border variabilities. Additionally, in some cases a larger value of threshold creates regression area at the image center, thereby leading to pseudo detection of lesions [94]. A triangular tessellation of the edge detected skin lesion image is computed using Delaunay triangulation [95]. The method combines edge based and region based segmentation algorithms. The boundaries of the triangle comply with the edges extracted wherein, heterogeneous regions are represented by larger and smaller triangles respectively. A heuristic threshold of 0.5 is used for merging the regions with a normalized boundary cost. The method reported an average segmentation accuracy of 0.896 [95].

Abbas et al. [50], proposed a melanoma border detection system using region based method with Hill Climbing Algorithm (HCA). The HCA takes the 3D histogram of the CIEL*a*b channels as the input and produces a set of peaks. HCA returns one color cluster label for the image and the corresponding histogram bins. The HCA helps in identifying the cancerous and non-cancerous skin by detecting the most relevant peaks globally. The peaks serve as seeds to the k-means clustering algorithm [50]. Mixture models and entropy based thresholding methods are used for segmentation of skin lesions [97]. The likelihood function of the mixture models are optimized using expectation maximization techniques to obtain roughly segmented lesions. Further, Otsu thresholding and morphological reconstruction algorithms are applied to refine the lesion segmentation process.

5.2.2. Soft computing based approaches

Soft computing based approaches are also used to classify the image pixels as belonging to ROI or background. Neural network and fuzzy based approaches are mainly used soft computing techniques for classification of pixels [98,99,114]. Evolutionary computing also forms a part of soft computing approaches. The classification of images is based on learning, human reasoning and evolution. These techniques in conjunction with medical image processing techniques improve the segmentation performance. Due to better adaptability, fault tolerance and optimal performance Artificial Neural Network (ANN) are the most prominent methods, which exploit the remarkable characteristics of Human Visual System (HSV) in case of image segmentation. The dominant model for color segmentation is Kohonen's Self Organizing Maps (SOM) [100].

Recently, convolutional neural networks have been adopted to increase segmentation accuracy of skin lesion images. The use of convolutional neural network in skin lesion analysis has garnered significant attention with commencement of the ISBI 2017 melanoma detection challenge with significant contributions in this regard. Qi et al. [102] used a fully convolutional neural network with a pre-trained VGG 16-layer net [101], with randomly initialized weights for skin lesion segmentation. The pre-trained network eliminates the need for a larger training data. Further, stochastic gradient descent is used for fine tuning the network [102]. Yu et al. [103] adopted residual learning techniques to train deep neural networks thus designing a Fully Convolutional Residual Network (FCRN) of more than 50 layers. The limited training data problem gets highlighted due to the presence of artifacts, poor contrast resulting in segmentation errors. FCRN with 50 layers outperformed the VGG-16, GoogleNet, FCRN-38 and FCRN-100 architectures resulting in a segmentation accuracy of 94.9% [103]. A 19-layer deep Fully Convolutional Network (FCN) is used for segmentation of skin lesions by Yuan et al. [104]. Image augmentation and pixel wise lesion mask prediction was adopted to solve the limited data problem. Additionally, the segmentation performance was improved by the use of techniques such as batch normalization, Adam optimization and Jacquard index based loss function [104]. A U-Net architecture based multitask Deep CNN was used in [105]. Limited availability of training data, presence of artifacts, and poor contrast degrades the performance of segmentation algorithms based on CNN, thereby facilitating the need for post-processing techniques such as level sets, conditional random fields etc.

The standard FCM frequently used in pattern recognition permits one bit of information to have a place with two or more classes. In fuzzy based hierarchical algorithm segmentation is performed by combination of CIEL*a*b color features and texture features. Optimal segmentation is obtained by splitting, local and global merging, followed by refinement of boundary [106]. Zhou et al. [107] proposed Anisotropic Mean Shift FCM (AMSFCM) which is effective and less time consuming providing superior segmentation results. In Mean Shift techniques the local density gradients are estimated using the radially symmetric kernels. However, implementation of Mean Shift is difficult due to the inadequacy of the kernels in dealing with irregular structures and noise. AMSFCM offers better solution in this regard due to the use of anisotropic kernels. Skin lesion segmentation using Dynamic Programming (DP) was proposed by Abbas et al. [108]. DP is used for determination of the lesion edges using a set of candidate points and cost function on radial profile points. A limitation of the method proposed in [108] lies in the background correction step. An improved version of DP for skin lesion segmentation was proposed in [109]. The improved DP utilizes the color and texture information in the CIEL*a*b color space. Ant colony optimization is used for segmentation of skin lesions in

[110]. The multidimensional graph representation of image serves as a platform for movement of ants guided by pheromone traces. Abrupt intensity variants are identified by moving ants leading to formation of segmented contours of skin lesions.

5.2.3. Deformable models

Deformable models form effective techniques in the field of medical image segmentation. Based on the techniques for tracking curve movement the deformable models are classified as parametric and geometric models. The parametric models explicitly represent the curves and surfaces during deformation in parametric form. The models are described by minimizing energy formulation or dynamic force formulation. Active contours form a part of parametric models. Active contours based segmentation algorithms have been used to segment the skin lesion images [96]. In active contour model the initial curve moves towards the ROI through deformation. The model also includes an external energy which drives the curve to the desired boundary. Active contours are capable of dealing with more complicated objects and are topologically inflexible. However, there exists few limitations such as, difficulty in dealing with large curvature boundaries, the curve initialization must be near the objects boundary, difficulty in dealing with topological changes during curve evolution, and bad edge localization for a small value of gradient, as the image gradient decides the stopping criterion. Few researchers have designed automatic curve initialization. For instance, in [111] automatic contour initialization is performed by binarizing the image with Otsu threshold reduced by 10 and choosing the closest object to the image center. A three step segmentation approach was proposed by Cavalcanti et al. [112], initially Otsu's segmentation is applied to multichannel representation of the dermoscopic image. The corresponding channel represents the maximum intensity variabilities between the lesion and non-lesion pixels. Further, the separability between the foreground and background is maximized by projection onto a color space inspired by Tsumura et al. [113]. The segmentation process is further refined by application of Chan-Vese active contours. This method contributes to the automatic initialization of Chan-Vese active contours. Chan and Vese model is an active contour model without edges. Topology adaptive snakes (T-snakes) were proposed in [116]. The snakes are characterized in terms of affine cell decomposition (ACID) of the image domain. It includes division of image into a collection of convex polytopes, consequently creating a mathematical framework that extends the capabilities of standard snake models.

The Gradient Vector Flow (GVF) is also used for skin lesion segmentation. Segmentation of skin lesions using classical GVF was proposed by Zhou et al. [134]. The distance between the curve centroid and ROI boundary was calculated to find the most similar edges. The model resulted in successful calculation of image based energies even in the presence of noise. The geometric models are based on curve theory evolution and level set method, thus offering solutions to most of the problems faced by parametric models. The topological changes are easy to control due to parameter independent evolution thereby generating curves that represent level set of a multidimensional function. The level set method and Chan-Vese methods are examples of Geometric models. The level set method overcomes the limitations of parametric models by the capability to handle topological changes during curve evolution. Zhen et al. [117], proposed a technique to model segmentation process as curve evolution. The level set method was used in the geometric models to facilitate computation. The curve is implicitly embedded in a higher dimensional level set function as its zero level set, reducing the complexity considerably. It is observed that lesion boundaries are traced considerably well eliminating the need for post-processing. However, the initial selection of the contour near object boundaries makes the entire process semi-automatic. The region based level set method using Gaussian probabilistic model was proposed by Silveria et al. [118]. A modified level set algorithm was proposed by Nourmohamadi et al. [119]. The results obtained by FCM clustering, Otsu, k-means clustering and other iterative methods were used for giving values to level set segmentation, thereby estimating the controlling parameters.

5.2.4. Other methods

Few other methods that were adopted for localizing the skin lesions are briefly explained in this sub-section. Fondon et al. [120] detected the ROI in the skin lesion image using Hill Climbing Algorithm (HCA) with CIE L*a*b color channels. The HCA detects local maxima of the clusters and associates the image pixels to the detected local maxima. The segmentation process is automatic and does not require prior knowledge of the clusters [120]. A non-parametric clustering technique that does not require initial knowledge of number of clusters is the mean shift algorithm. It employs an iterative hill climbing process to the nearest density point which is stationery, thereby converging the local maxima after few iterations. The mean shift algorithm results in a cluster where image data is portrayed in feature space [121]. A fixed window size is used by the algorithm, thus a small value of window size results in cluster over-splitting and a large value of window size results in excessive merging. Therefore using an adaptive value of window size is termed as adaptive mean shift. Adaptive Wavelet Network (AWN) and Fixed Grid Wavelet Network (FGWN) are two types of wavelet networks. The former is continuous wavelet transform whereas, the latter is a discrete wavelet transform. The application of AWN is limited due to several reasons such as sensitivity to initial values, complex calculations etc. In AWNs, introductory estimations of system parameters including weights of neurons, wavelet scales are chosen arbitrarily or utilizing different techniques. These parameters are then redesigned in the learning stage using techniques such as back propagation, and gradient descent whereas, in a FGWN, the wavelet numbers, scale and shift parameters can be determined well in advance and the weight coefficients are calculated using least squares technique. The FGWN algorithm is given in detail in [122]. In [123], Cohen-Daubechies Feauveau biorthogonal wavelet is applied on the blue-channel of the lesion image and it was inferred that the second approximate wavelet produced better results.

Qui et al. [124] proposed the Information Theoretic Dictionary Learning (ITDL) by maximizing the mutual information measure that can be used for clustering tasks. This is performed by selection of k-value such that dictionary compactness, representation and discrimination are maximized. The feature dictionary and k-value is optimized further for segmentation of the image [124]. An unsupervised method of ITDL is used to select constant number of k-atoms from Non-Negative Matrix factorization (NMF) learned dictionary by Flores et al. [125]. An improvement to the method in [125] was performed in [126], to optimize the segmentation of skin lesions, by adaptively selecting the number of dictionary atoms for different images. NMF utilizes the texture variations in the image to produce a sparse feature set represented in the form of an undirected graph. The normalized graph cut algorithm is used further for creation of binary masks. Robustness to data outliers with the assumption that the skin lesions do not touch the image corners is the major strength of the method proposed in [126]. In [127], a narrow-band graph partitioning is used to improve the computation efficiency of the segmentation algorithm.

Lesions are segmented using homogeneity constraints on the region based snakes consequently, the lesions are merged depending on the gradient information and centroid distance. A brief overview of the segmentation algorithms that can be used for der-

Table 2
Methods of Segmentation for dermoscopic images.

Segmentation Method/Broad Categorization	Segmentation Method/Specific Categorization	No. of Images	Evaluation Metric	PT	Comments
Thresholding Based Methods	Thresholding [128]	426	NoMSL: 84.5% Prec., 88.5% Recall; MSL: 93.9% Prec., 93.8% Recall	NA	Computationally inexpensive, Selection of threshold is crucial wrong choice may result in over/under segmentation.
	Thresholding [51]	367	16.9% XOR	0.2s	
Region Based Methods	Region Merging [129]	60	93.06 TDR; 3.03 FPR	NA	Accurate segmentation of regions having the same properties and provides flexibility in selection of seed point
	Iterative Stochastic Region Merging [130]	60	Segmentation Error- 9.16%	6s	Usage of merge splitting prior to region growing results in sharper edges and results in blurry images.
			True Detection rate- 93.06%		Difficult to decide stopping criteria.
			False Positive rate- 3.03%		
Fusion Based Methods	Thresholding + Active Contour [131]	250	10.82% Difference between GT and SI	NA	Avoids post processing and peculiarities of the participating segmentation algorithms can be exploited leading to robust segmentation
	Thresholding+ Active Contour [112]	152	90.07% SE, 99.11% SP, 15.60% XOR	NA	
	HCA+ Region Based Method [50]	100	94.25% TPR, 3.56% FPR, 4% EP	9.52s	
	Fusion Thresholding [132]	90	8.79% XOR	0.1s	
Deformable Models	Chan-Vese [96]	408	Subjective Evaluation 94.36%	49.12 min for 385 images	Can simplify analysis by minimizing the amount of pixels from and preserves the adequate structure of the objects
	Region Based Active Contours [133]	175	Single contour Initialization: 8.38% EP; Multi-contour Initialization: 4.10% EP.	17.89s	Noise may result in erroneous edges selection of gradient function should be properly calibrated.
	Mean Shift GVF [134]	100	86% SE; 99% SP	NA	
Soft Computing Based Approaches	Co-operative Neural networks [135]	100	Greylevels:0.16 XOR	NA	Deals with large complex search spaces where minimum knowledge is available of the objective function
	Evolution Strategies [136]	111	45.77 to 84.71 Error Rate Reduction	15 min	Effective and automatic segmentation techniques
	Fully Convolutional Residual Network [103]	900 Training 350 Testing	0.911 SE, 0.97 SP	0.52s	
	Convolutional Neural Networks [104]	900 Training379 Testing	0.847 JI	0.14s	
	Dynamic programming [108]	240	BM: 8.6% EP; M: 5.04% EP; BCC: 9.0% EP; MCC: 7.02% EP; SK: 2.01% EP; Nevus: 3.24% EP.	12.65s	
	Improved Dynamic Programming [109]	100	94.64% SE; 98.14 SP; 5.23 EP	2.5s	
Other Methods	Dictionary based Method [126]	152	16.89 Average XOR Error	NA	Unsupervised segmentation technique robust to data outliers, and sensitive to non-uniform illumination

PT – Performance Time.
NA – Not Available.

moscopic images is presented in Table 2. The outcomes and views associated with each of the methods have been highlighted.

6. Dermoscopic feature extraction

By extricating features, we contract down the image information to an arrangement of components which ought to be vigorous

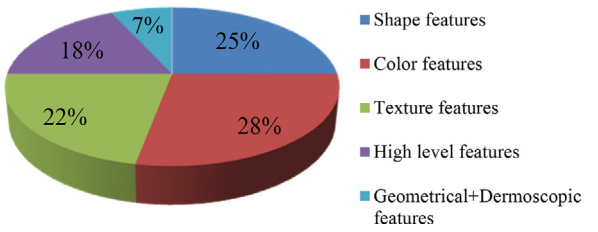

Fig. 2. Illustration of feature distribution used in dermoscopic studies in the literature.

against elements, such as lighting, camera position, commotion, and absence of clarity. A number of studies have been carried out for the features from the entire image or from the segmented region. The following sub-sections provide an insight of the various features extracted from the dermoscopic images till date. A distribution of the feature categories is illustrated in Fig. 2.

6.1. Pattern analysis

The pattern analysis method was updated in the Consensus Meeting of Dermoscopy (CNMD) in 2000 [137] and pristinely introduced by Pehamberger et al. in 1987 [138]. Pattern analysis identifies melanocytic lesions and the caliber of malignancy utilizing local and global patterns [137]. Local patterns of dermoscopic structures incorporate pigment system, dabs and globules, streaks, blue whitish shroud, relapse structures, hypopigmentation and vascular structures present in the distinctive regions of the same lesion. Global patterns sanction an expeditious preliminary categorization of PSL prior to the detailed assessment. It includes reticular, globular, cobblestone, homogeneous, stardust, parallel, multicomponent, lacunar and unspecific patterns. It was deemed superior to the other three scoring dermoscopy algorithms [138] (ABCD rule, & point checklist, Menzies method) and exhibits highest diagnostic precision [139,140].

6.2. ABCD rule

The ABCD rule of dermatoscopy was the second algorithm after pattern analysis [141]. Four criteria were found to be significant factors for melanoma diagnoses after performing a multivariate analysis of 31 dermoscopic criteria. It is a semi-quantitative scientific methodology that gives points for the criteria which include Asymmetry (A), Border (B), Colors (C) and Differential structures (D) identified in a PSL. Each identified criteria is multiplied by a weight factor to establish a Total Dermoscopic Score (TDS) as given in equation (1).

$$TDS = 1.3 * A + 0.1 * B + 0.5 * C + 0.5 * D \quad (1)$$

A lesion is considered benign for a TDS score lesser than 4.75. For an intermediate TDS value of 4.75–5.45 it is regarded as possible melanoma and a score above 5.45 indicates probable melanoma.

6.3. Menzies method

Introduced by Menzies et al. [139] in 1996, the method probes for negative features. For a lesion to be relegated as melanoma at least one positive feature must be found. Negative features include patterns that are point or axial asymmetric and presence of a solitary shading (gray, ebony, blue red, tan and dark brown). The nine positive features include blue white veil, multiple brown dots, pseudopods, radial streaming, depigmentation, peripheral ebony dots/globules, multiple hues, numerous blue/dark spots and expanded network.

In some approaches the asymmetry index is obtained by taking the asymmetry score as the average between two scores obtained by score obtained from the non-overlapping area of the major and minor axis and that obtained by color (in terms of histogram of the RGB planes) [140], based on geometrical measurements on the whole lesion [144].

6.4. Seven Point checklist

The 7 point checklist assign a score based on 3 major and 4 minor criteria. Atypical pigment network, blue-white veil and atypical vascular pattern are the 3 major dermoscopic features. Minor features include irregular streaks, irregular pigmentation, irregular dots/globules, regression structures. To score a lesion, the nearness of a major criterion is given 2 points and that of a minor model is given 1 point. On the off chance that the aggregate score is more prominent than or equivalent to 3, the lesion is named as melanoma [145,146].

6.5. CASH algorithm

The CASH (Color, Architecture, Symmetry, Homogeneity/Heterogeneity) algorithm is designed as simplified form of pattern analysis. It includes a feature architecture not utilized by any other scoring algorithm. Architecture refers to the organization of the lesion in terms of dermoscopic structure and colors. Since melanoma exhibits a characteristic of highly disorganized structure as compared to benign lesion it is utilized as a relegation measure. CASH algorithm is found to be commensurable to other well organized method [147]. Presence of light brown, dark brown, ebony, red, white and blue scores 1 point. Mono-axial symmetry and biaxial asymmetry are given 1 and 2 points respectively. Homogeneity/Heterogeneity includes networks, dabs/globules, blotches, relapse, streaks, blue-white shroud and polymorphous blood vessels. Each of these structures is given 1 point. Benign lesions incline to have one or two of these seven dermoscopic structure, whereas melanoma often have three or more structures. A total score of eight or higher relegates the lesion as suspicious for melanoma.

6.6. Shape features

Shape features aid in assessing the asymmetry of the lesion and the irregularity of the border. Melanoma skin lesions exhibit certain shape features that distinguish melanoma from benign lesions. In order to calculate Asymmetry Index (AI) the lesion is folded along its principal axis of inertia [148]. The asymmetric lesion shows a consequential disparity between the two moieties of the lesion, compared with the symmetrical lesion [149,150]. In some cases the size function which gives the qualitative measure of asymmetry is used [58]. Eccentricity the quantitative measure AI indicates the elongation of lesion [152]. The AI is calculated as in equation (2).

$$AI = \Delta A/A \quad (2)$$

Where ΔA is the non-overlapping area difference and A is the total area of the lesion. Other parameters giving the asymmetry measure of lesion are circularity index ($4\pi A/p^2$) [79,149], equivalent diameter ($4A/\pi$) [153,154], the fragmentation index is similar to the circularity index, it is measure of regularity of border and assigns a unity value for a circular lesion [155], aspect ratio. Compactness is used to assess the degree of similarity to a circle [156], lengthening indices are used to determine anisotropy degree of lesion [70], principal axes of inertia [157], major axis by bounding box method [158], best-fit ellipse, and Fourier transform are the various approaches to determine symmetry. Patel et al. [159] used manual

method for surface area measurement by placing the lesion location to be photographed in 1 cm^2 box, the histogram function was used to calculate the number of pixels. Although this method is less expensive, the calculation of lesion area can be an arduous task and prone to error if care is not taken [159].

Border irregularity is estimated as ratio of the square of the perimeter to the area of the tumor [160]. Bono et al. [161] defined border irregularity as smoothness by calculating ratio between perimeter of the curved frame of the injury and the lesion edge [161]. Conditional entropy also known as sequence based entropy takes the summation of products of joint probability and conditional probability. Conditional entropy does not take into record the relative positions of the components of sequence and hence it is not a good measure of irregularity [162]. Compactness ($p^2/4\pi a$) is sensitive to shape and margin of the lesion. The sensitivity and specificity in classifying the lesion into malignant and benign was 74% and 75% considering fractal dimension as a measure of border irregularity [162]. In order to measure lesion border irregularity, features such as least, greatest, normal, and variance responses of the slope administrator applied on the intensity image are utilized [163]. Requiring a lesion to be more prominent than 6 mm for diagnosing melanoma could bring about pseudo classification of lesions. The in-situ melanomas are often smaller than 6 mm [156]. This indicates that, the criterion for greatest diameter of the lesion is to be modified. The usefulness of ABCD system for recognizing melanoma from benevolent pigmented injuries has not been definitively portrayed [165]. Fourier descriptors due to their invariant nature are used to characterize the shape of the lesion [166]. An assessment of the border irregularity is also obtained by wavelet transform [167,168], and Fourier transform [169]. Kasmi et al. [170] used the third order spline function and computed the fitting error for each of the lesion sub-contours to determine the border irregularity.

6.7. Color features

Pixels inside the lesion fringe attribute to the color based features [171]. Variation of red, green and blue components gives the tumor texture. Color features are mainly calculated predicated on the statistical characteristics quantifications on RGB planes and relative color spaces such as HSV and CIE L*u*v which have the property of being invariants to illumination intensity and also allow decoupling of chrominance and luminance. It includes the standard deviation of RGB channels [172], mean reflectance by lesion in the visible and near infrared region [161], relative chromaticity [139], KL transformation for extraction of features that have immensely colossal discriminant power [142], chromatic differences [173], average RGB values [159], and most proximate neighbor approach [174]. Few researchers have exploited color spaces such as JCh [175], CIEXYZ [176], HVC [177], CMY [178], YUV [178] to obtain better lesion to skin discrimination capability. Spherical coordinates and IHS coordinate reparation are used by Wighton et al. [179]. A total of 30 features for each pixel by applying a series of Gaussian and Laplacian Gaussian filters to each color channel of the CIEL*a*b color space were obtained [179]. Color variegation involved the usage calculation of minimum, maximum and standard deviation of the selected channel such as CIEL*a*b color spaces [172], Barata et al. [172] tested 6 color spaces and evaluated the appropriation of colors in an image as a likelihood dissemination.

Histogram features from relative color image objects include mean, standard deviation, skewness, energy, and entropy [155]. Color histograms are translation and rotation invariant, thereby widely used to analyze the skin lesions [181]. Xie et al. [182] used a multivariate histogram consisting of joint distribution of color channels to determine the color variegation. The presence of more than three colors and specific colors in the PSL quantifies malignancy. Few researchers have adopted a color palette approach and consequently trained a classifier to recognize colors in the lesions [183,181]. Specific colors such as blue and red are determined by using the hue component and clustering [185,186]. Iyatomi et al. [187], determined the border color gradient using the luminance and blue channels average for eight equiangular regions. The difference between the lesion pixel value and surrounding skin pixels average value gives a measure of relative color difference irrespective of the uneven illumination effect, thereby used as a color feature [188]. Relative color difference between the inner and outer lesion peripheries reveals significant information about the lesion. Celebi et al. [152] obtained a set of 108 features by computing the mean and standard deviation for 6 color spaces for determining the relative color difference between the inner periphery, outer periphery and the lesion. The discrimination between benign and malignant lesion is also computed by calculating the color asymmetry feature. Quantification of the color asymmetry is obtained by computing the Euclidean distance between the symmetrical lesion pairs [165].

6.8. Texture features

A pigmented skin lesion possess visible form of texture. The texture features that relate to human visual observation are coarseness, contrast and directionality. Texture is homogeneous for human visual system [189]. Statistical, structural and transform based methodologies form the three main classes of texture feature extraction [190]. The statistical approach basically consists of image intensity domain, and mathematical domains. Histogram, co-occurrence matrix [190,191], run length and gradient matrix [192] form a part of image intensity domain. Some researchers used gray level co-occurrence matrix (GLCM) [193,152] wherein, mapping of gray level co-occurrence probabilities in view of spatial relations of pixels in various angular directions is performed [194]. Noticeable components extricated utilizing GLCM are contrast, correlation, homogeneity, energy, and entropy [194,195]. Garnavi et al. [167] used tree-structured wavelet decomposition for texture feature extraction, RGB and luminance color channels were used for processing. The Generalized Co-occurrence Matrices (GCM) take into account the correlation between the channels, GCM are expansion of co-occurrence matrix to multispectral pictures [197,198]. Few of the GCM features include variance, group shade, cluster noticeable quality, most extreme likelihood, autocorrelation, divergence, homogeneity and so forth. Textures measures used correlation average at advanced pixel spacing for recognition of sporadic shade system in early dangerous melanoma [199].

The idea of computing the statistics of neighboring pixel pairs is modified and improved in several ways. For instance, the Local Binary Pattern (LBP) performs binary classification of the pixels and computes the neighboring pixel statistics. A completed LBP is used in [200] wherein, differences between the center pixels is encoded as a binary pattern and the corresponding histograms are used as feature descriptors. Gradient histograms have also been used to characterize the texture of the skin lesions. Barata et al. [172] computed gradient vector using Sobel filter on a gray level Gaussian filtered image. Histogram of oriented gradients computes the occurrence frequency of gradient orientations [200]. Transform based features have been utilized for extraction of texture features for skin lesion images, these include Fourier Transforms [186,201], Gabor Filters [200,202], Wavelet Transforms [167,203], and Laws energy masks [204]. These features utilize the spectral energy in the frequency domain to characterize texture. The Scale Invariant Feature Transform (SIFT), considered as the most popular patch descriptor computed in the luminance image describes the lesion

shape around the point using gradient histograms. A comparative performance of three color descriptors is given in [205].

6.9. High level features

Certain dermoscopic structures are utilized by dermatologists for differentiation between the lesions in integration to prevalent features. Braun et al. [206] estimated the paramountcy of granularity for dermoscopic examination of melanoma and concluded that eccentric granularity lesions require surgical excision. Granularity is the accumulation of minute, blue-gray granules in dermoscopy images additionally kenned as peppering [207]. Blue white veil is detected by color analysis tasks in [208]. Dots kenned as structure less areas [38,209] are distinct minuscule circular colored spots representing accumulated localized pigment. Melanoma color pixels are located on the interior of the lesion. Dark areas in melanocyte lesion and peripheral shaped dots give a denotement of malignancy [138,210]. Brown globules correspond to melanocyte accumulation at the junction and upper epidermis. Few other high caliber features include blotches [209], white areas, regression structures, streaks [209,211], and pigment networks [212]. Thus these high caliber features should be embedded in the diagnostic system to increment the efficacy of melanoma diagnosis.

An extensive review of the detection of dermoscopic patterns is found in [213]. Abbas et al. [175] identified seven classes of dermoscopic patterns using color and texture features to classify melanocytic and non-melanocytic lesions achieving an average sensitivity and specificity of 89.98% and 93.75%. Maglogiannis et al. [171] used non-linear inverse diffusion for detection of dots/globules to determine the impact on classification performance. Changes in lesion features over a period of time (evolution) indicates malignancy. Skr et al. [214] quantified morphological changes in the lesion by using PCA and a medical registration technique termed as stochastic gradient descent. Quantifying the skin lesion elevation aids in skin lesion classification as tumor thickness indicates the depth of malignancy. Three dimensional digital imaging of the skin lesions could be used in this regard. The gap between the lesion base and its corresponding surface indicating lesion thickness is measured in [215], utilizing 3D skin surface image. However, to the best of our knowledge due to the complexity involved and limited availability of the datasets with skin lesion images obtained at different periods of time, techniques that measure the skin lesion elevation and evolution are few as mentioned above, thus there exists a scope for designing efficient algorithms in this regard.

7. Feature selection

Feature selection involves optimized subset of features providing the highest discriminating power eliminating redundancy, irrelevancy and simplifies computation when employed to classifier. The optimality of feature subset is quantified by an assessment criterion. Predicated on the evaluation criteria, feature selection involves three categories which include the filter model, the wrapper model and the hybrid model which is a coalescence of the former models. The wrapper model is sumptuous compared to the filter model. The major distinction between the first two models is that the filter model utilizes the general attributes of the information to select optimal feature subgroup and does not require any cognition algorithms whereas, the wrapper model utilizes the cognition algorithm and endeavors to ameliorate the performance of the cognition algorithm utilizing methods such as greedy or genetic algorithm. The gain ratio predicated feature selection by Garnavi et al. [167] results in considerable change in the framework execution and an incredible lessening in the measurement of the component vector, and also the required time for assignment. It uses the ranker inquiry technique to rank and sort the component features. Fisher score rankings is utilized by Sheha et al. [194] for selection of highest score features from the input dermoscopic images. Twelve features were selected from 23 features utilizing fisher score [194].

There are many methods available for feature selection, the most commonly used method is the Principal Component Analysis (PCA). The PCA technique also kenned as Karhunen-Loeve (KL) transform, it has the ability to discriminate directions with the largest variance in the dataset. PCA predicated feature selection lessens the dimensionality of the component space thereby reducing the computational cost of analyzing incipient data. Principal components are the extracted uncorrelated components and are estimated from Eigen vectors of the co-variance or the correlation matrix of the pristine variable. Principal Feature Analysis (PFA) exploits the structure of the vital segments of an arrangement of features to pick the important features (maximum variability) [216]. Wighton et al. [179] used Linear Discriminant Analysis (LDA) for feature subset selection. Few heuristic search algorithms such as ranker [128], incremental step-wise [180], and random selection [152] adopt a sequential, complete or random search strategy.

Other search strategies include Sequential Forward Selection (SFS) [217], Sequential Backward Selection (SBS). Feature ranking and SFS are proposed in [218], in order to extract critical features ranking of features is done according to their importance and then SFS is applied to features that are less important. In order to avert the nesting effect suffered by SFS and SBS, the plus-l-minus-r was developed in 1978 by Kittler [219]. The floating search method treats the nesting quandary better compared to the former approach. The plus-l-minus-r method requires the designation of parameters (l, r) whereas the forward/rearward steps are determined dynamically in the floating search methods according to the criterion function [219,220]. The floating search methods include Sequential Forward Floating Search (SFFS), Sequential Backward Floating search (SBFS), SFFS commences with a null feature set. At each step, the best feature is selected that satiates the criterion function simultaneously and the worst feature concerning the criterion is eliminated. SFFS proceeds dynamically incrementing and decrementing the number of features until the desired set dimension is reached. SBFS proceeds analogous to SFFS with a full feature set at the start. The classification performance reached is above 65% with SFFS and SBFS accommodating the subset size of 10 and 15 respectively, and there was a degrade in the performance for feature subsets of size 20 [221]. Albeit, floating methods are considered definitely intellective, but they are suboptimal and there is no guarantee that they yield better results.

In integration to these, some filter predicated methods are utilized. Filter methods are commensurably more expeditious but inclines to choose subsets with a high number of components thus a limit is required to select a subset. RELIEF algorithm [222] estimates the nature of ascribes as per how well their qualities recognize occasions that are proximate to each other. The RELIEF algorithm is circumscribed to 2 class quandaries but can deal with discrete and perpetual data. An extension to RELIEF algorithm is ReliefF. It deals with multiclass problems and also deals with incomplete and strepitous data [223]. The Mutual Information predicated Feature Selection (MIFS) selects those individual elements and the class marks that have the common data that measures the discretionary conditions between the arbitrary variables [224]. The Fast Correlated Based Filter (FCBF) is predicated on relegation of high dimensional data [225]. INTERACT algorithm is same as FCBF but includes the consistency feature which denotes how significantly the elimination of the feature effects consistency. It employs backward elimination to abstract those features with no or low consistency contribution [226]. Correlation based Feature selec-

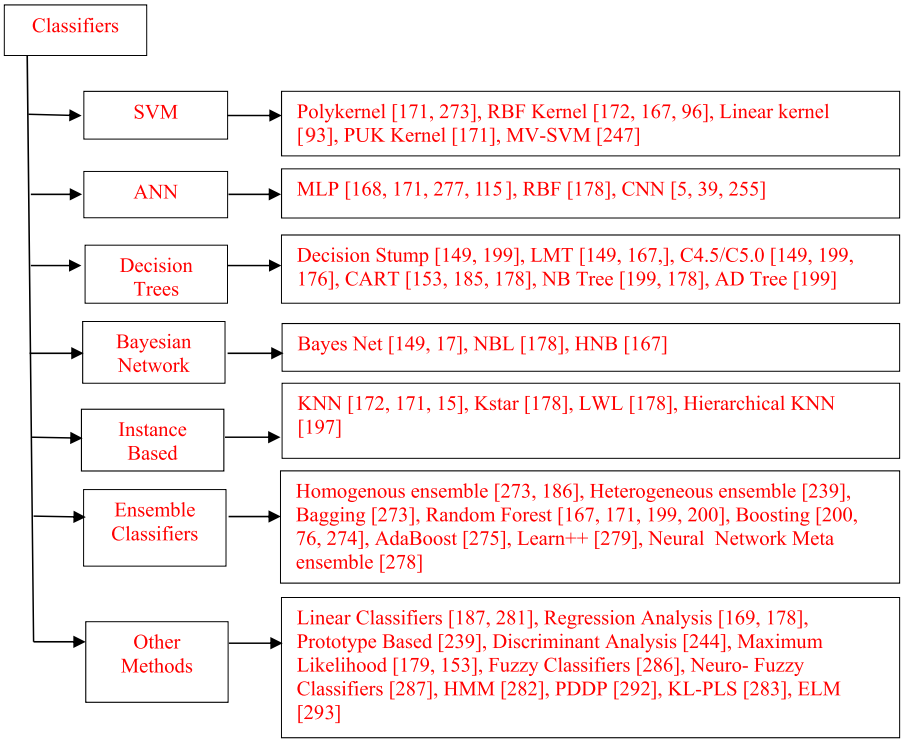

Fig. 3. Methods for classification of pigmented skin lesions.

tion (CFS) utilizes a heuristic search strategy and feature subsets are ranked according to the features that are highly correlated and uncorrelated with each other. Correlation based expert system filter carried out in a backward selection method is utilized for feature selection in [148]. It uses a relationship based on heuristic to assess the value of components. The heuristic considers class name along with the caliber of relationship between them. CSF has higher cardinality and provides adequate detection of interacting features [228]. Clustering tasks turns out to be a conundrum using filter methods with a minimum degree of optimality [226].

Wrapper methods rely on the execution of an unmitigated classifier to assess the nature of quality of features. Forward and backward search strategies can be applied. Customarily, non-exhaustive search algorithms like genetic algorithm, greedy stepwise are often used since they are computationally inexpensive [230]. In the wrapper approach, the induction algorithm is utilized as black box. The dataset consisting of the training set and the feature set is utilized as the input to the induction algorithm [231]. The Support Vector machine-Recursive Feature Elimination algorithm (SVM-RFE) [232] relies on the performance of the SVM classifier. Five features of SVM-RFE were shown to be optimum for the purpose of malignancy relegation with border irregularity considered as the most consequential feature [233]. RFE is much more robust to data over lifting including combinatorial search [231]. Overfitting issues rarely occur using SVM when compared to other algorithms implementing empirical risk minimization principle. However, if conventional RFE algorithm is utilized as wrapper, it is necessary to utilize the SVM classifier in order to evade the RFE to turn it into a computationally extravagant filter method [79]. The quantity of elements held by the feature selection algorithm is a paramount parameter. By inspecting the overall performances medium sized subsets give the optimum relegation performance. The melanoma recognition rates reduce with larger subsets which might lead to over fitting. More diminutive classes of feature may cause an error in relegation. Therefore feature selection algorithms should be evaluated with marginally different data for all algorithms with a standard classifier in order to obtain performance estimation.

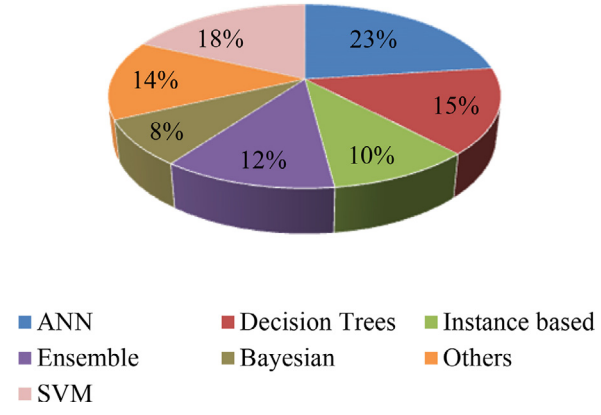

Fig. 4. Illustration of classification methods used by existing diagnostic methods.

8. Classification

Classification constitutes the last stride of CAD conclusion framework to decide the PSL class [239]. The chose elements are broken down and sorted out into classes. Preparing and testing data form the two periods of supervised classification. The procedure of utilizing known substance having a place with determined classes and making a classifier on such premise is known as training. In the following testing stage, the prepared information is utilized to decide class for the dermoscopic lesion image. A brief review of the well-known methods as well as techniques based on state of art classification methods used in computer-aided melanoma demonstrative frameworks are explained. The Fig. 3 illustrates the classification methods used in PSL detection. Fig. 4 depicts the frequency of the classification methods used in literature.

8.1. Instance based classifiers

Instance based classifiers do not initially build a learned classifier from the trained instance, but performs classification by comparing a query instance to a known instance from the training set. Distance between the instances is used as a comparison metric. The K-nearest neighbor (K-NN) [99], is a simple algorithm that stores all available cases and relegates incipient cases predicated on a kindred attribute measure. K-NN was initially presented by the scientists E. Fix and J. Hodges in 1951 [234]. K designates how many most proximate neighbors are to be considered to define class of a sample data point. K-NN does not make any posits on the underlying data distribution and hence it is termed as non-parametric method for relegation. A consequential aspect of K-NN classifier is that it lacks generalization and does not require earlier intellect of the appropriation but rather depends on a preparation set of items with kenned class to make decisions. This is as opposed to different strategies like SVM where you can dispose of all non-support vectors with no quandary.

$$d = \sqrt{\sum_{i=1}^{k} (x - y)^2} \tag{3}$$

The distance function for continuous variables includes Euclidean and Manhattan, illustrated in Eqs. (3) and (4) respectively.

where x_i and y_i are the data points

$$d = \sum_{i=1}^{k} |x - y| \tag{4}$$

A small variation in value of K increases flexibility and vice versa. The classifier utilized by Ramlakhan et al. [235] could perceive benign lesions superior to suspicious ones with sensitivity of 80.5% for benign and 60.7% for malignant lesions.

In hierarchical leveled design, singular classifiers can be amalgamated into a structure akin to a decision tree. A hierarchical K-NN classifier was used for classification of skin lesions in [197] with one classifier at the top level and two classifiers at the bottom level. The two classifiers at the bottom level are trained utilizing only the images that have been correctly relegated by the top classifier consequently relegating them into one of the 2 or 3 demonstrative classes providing a precision of 74%. Ensemble of classifiers surpass any of its individual components [236] resulting in ameliorated apperception precision [237]. Numerous apathetic learning algorithms are subsidiaries of K-NN classifiers such as Lazy CL [238]. In 1970's K-NN was utilized as non-parametric method and has been used in measurable estimation and pattern apperception. K-NN is a simple classifier and works well for rudimental apperception quandaries. The major drawback is that, it is a slothful learner and does not imbibe anything form the training data. Distance computation and sorting of the training data can be slow in case of astronomically immense number of training samples. Additionally, the transmutation in the adjustable parameter K reflects vicissitudes in the presaged class label. Kstar classifier differs from the other instance based classifiers by the use of the distance based entropy function. LWL classifier assigns instance weights using the instance based algorithm and is used for classification and regression tasks [178].

8.2. Support Vector Machines (SVM)

SVM was first introduced in 1992 by Vapnik [240], SVM is a set of cognate supervised learning method for relegation. It implements the conception that feature vectors are non-linearly mapped to a high dimensional element space. SVM are considered as maximum margin classifiers, because they curtail the empirical relegation error and increase the geometric margin. Considering input data as two set of fortification vectors in an n-dimensional space, an SVM constructs a dissevering hyper-plane which enlarges the margin between the two data sets. Margin refers to minimal distance between the most proximate data point and the dissevering hyper-plane. SVM seeks for an optimal disuniting hyper-plane where the margin is maximal. In order to use SVM to a pattern recognition task conversion of the input data to a higher dimensional space m_1 from a lower dimension space m_0 is performed. On the basis of the kernel definition different machine learning models can be built using SVM. In order to find an optimal hyper-plane in the feature space for inner product, kernel mapping function illustrated in equation (5) is utilized, if the symmetric part fulfills the Mercer's hypothesis [241].

$$k(x, x_i) = \phi^T(x)\phi(x_i) \tag{5}$$

where ϕi is a set of transformation function ϕ_j

$j = 1, 2 \ldots m_1$

x_i is the i^{th} known training sample

SVM algorithm involves accession of a convex cost function without local minima and evaluation of model utilizing support vectors to relegate test data set. The performance evaluation involves tenaciousness of the error rate as test data size inclines to illimitability [242]. Ramezani et al. [154] used SVM with Radial Basis Function (RBF) kernel as a classifier due to the flexibility of transmuting the parameters of the data models for skin lesion relegation. In RBF the stronghold vector calculation consequently decides focuses, weights and edge to minimize an upper bound on the expected test mistake [154]. A polynomial kernel can perform the same operations as the prevailing feature extraction algorithms. The SVM algorithm was implemented by Maglogiannis et al. [244] utilizing numerous kernel functions, the dimensionality of the quandary was reduced by eliminating a few elements concerning standard deviations and least or most extreme estimations of components were disregarded [244]. The best execution was accomplished utilizing the exponential radial substratum function with sigma value of 7 resulting in a precision of 91.84%, specificity and sensitivity of 91.87% and 91.30% respectively [244]. Torre et al. [245] concluded that SVM execution differs significantly, contingent upon the kernel type used. Using shading elements and manually segmented images, the overall apperception rate goes from at least 59.0% for the Gaussian kernel to a greatest of 76.0% for chi-squared portion [245].

SVM attains apperception results commensurable to those obtained by adroit clinicians [245]. SVM is less prone to over fitting compared to back propagation neural system that actualize exact risk minimization. Neural systems have various solutions connected with nearby minima and consequently may not be vigorous for various cases while SVM disseminates a novel arrangement, since the optimality scrape is arched. This is favorable in contrast with neural networks, SVM provides flexibility in the selection of kernel consequently providing a coalesced framework for developing architecture of many machine learning models. There are no theoretical bounds on the generalization error. SVM is expected to be more precise than human visual screening and hence utilized in medical domain widely [242]. By picking a proper speculation grade, SVMs can be powerful regardless of the possibility that the training test has some bias. The major drawbacks of SVM are the selection of melanocytic and non-melanocytic patterns. The Majority Vote-SVM (MV-SVM) was built using the traditional SVM. The majority vote algorithm overcomes the problem of manually adjusting the weights at each run time [247].

8.3. Discriminant analysis

Discriminant analysis is a statistical technique to relegate objects into totally unrelated and comprehensive groups predicated on a set of quantifiable objects features. In order to assess the adequacy of relegation discriminant analysis may be utilized. It identifies the amalgamation of the variables that best characterizes the distinction between the gatherings. The assessed coefficients and resultant discriminant function can be habituated to consign cases [248]. Discriminant analysis is utilized as probability measure in pigmented lesion diagnosis in a multi-classifier component, predicated on the features selected by univariate analysis. Discriminant analysis achieved a relegation precision of 97% in [244] for radial magnification phase of dysplastic lesions. However, it requires astronomically immense training samples. The Probability function and Fisher's linear discriminant function are two common discriminant rules. Fisher proposed boosting the refinement between the convenient, normalized by a measurement of the inside class scatters. The fisher linear discriminant is characterized as the linear function $w^T x$ that amplifies the criterion function [249] illustrated in Eq. (6).

$$J(w) = \frac{|\mu_1 - \mu_2|^2}{s_1^2 + s_2^2} \tag{6}$$

where $\mu_1 - \mu_2$is the distance between the projected mean values and ${s_1}^2 + {s_2}^2$ is the within class scatter. Burroni et al. [99] used discriminant analysis function for every lesion in the test set, it was allocated to a melanoma group if it satiates a threshold criterion. Quadratic discrimination function makes utilization of unequal multivariate mundane distributions among groups. Discriminant analysis may not retain the involute structure in the data needed for relegation if the distribution is significantly not Gaussian in nature.

8.4. Artificial Neural Networks (ANN)

An Artificial neural system is an information processing paradigm that is displayed by the way organic sensory systems process data. It is made out of cosmically gigantic number of exceptionally interconnected processing elements kenned as neurons working in unison to solve categorical quandaries. It is a massively parallel distributed processor. It resembles the brain in two aspects. A neural system comprises of units orchestrated in layers, which change over information vectors into some yield. Every function takes an input applies a function to it and then passes the output onto the following layer. The ANN learns in directed way, the information is displayed to the system which will then figure a yield predicated on this information. Learning phase involves application of the weights to the signals and further adjusting these weights to habituate a neural network. This is a repetitious process which perpetuates until the determined condition is met. In the input layer the condition of neuron is resolute by the input variable, the state of neurons for the hidden and output layer are evaluated by the state of the precedent layer. ANN coalesces artificial intelligence and information processing thus sanctioning input data of PSL to be processed. This integrated system should be proficient of detecting and relegating an incipient PSL on the substructure of the type of input received [251]. In 1994 Binder et al. [252] first applied ANN for 200 PSL images and obtained a lower value of sensitivity. Further in 1998 he obtained 90% of sensitivity and 74% of specificity. It was additionally observed that ANN can be trained adequately to segregate between benign and malignant PSLs [252].

Multilayered feed forward network with back propagation training algorithm is utilized to relegate digital images into fine-tuned categories utilizing a hyperbolic tangent function. The size of the training set and test set are maximized in order to get the best relegation network. Back propagation is a gradient descent technique that minimizes the squared fault between the genuine output of the system and the craved output. Sheha et al. [194] used GLCM for feature extraction and obtained a 100% training and 92% testing precision utilizing the traditional Multilayer perceptron (MLP) for segregation amongst malignant and melanocytic nevi dermoscopic pictures [194]. MLP is a feed forward system fit for inciting non-linear boundaries. The strength of multilayer perceptron is that there are a few layers of versatile weights and non-linear activation function [115,277]. Albeit, the algorithm has major drawbacks such as slow computing speed, and probability of being caught in nearby minima, PCA and cross entropy functions can be acclimated to surmount them respectively [253]. CAD software programmers used ANN as a first choice for relegation quandaries [254]. ANN has the ability to handle data corrupted by noise redundancy and having nonlinear decision boundaries. Since, ANN classifiers provide reduced error rates compared to statistical approaches they are potent and flexible designates for mapping inputs to discrete classes, which can be mimicked to the mapping of a set of symptoms to a set of possible diagnostic classes consequently, providing a robust approach to deal with medical diagnosis issues [255]. Additional knowledge of the dataset cannot be obtained from a neural network as the model parameters are not directly interpretable [256].

Deep learning algorithms, powered with the capability to perform involute computation with large datasets, have exceeded human performance capabilities in tasks such as object recognition, playing games etc. The most popular architectures used for image classification tasks include the Convolutional Neural Networks (CNN). CNN's have led to breakthroughs in medical image analysis tasks. Few researchers have employed CCN's for classification of melanocytic lesions, with the aim of exploiting their powerful discrimination capability. CNN architectures used for computer vision tasks include QuocNet, AlexNet, Inception (GoogleNet), BN-Inception-V2, Inception-V3. A brief history of the evolution of CNN can be found in [257]. Codella et al. [258] integrated CNN's, sparse coding and SVM for recognition of melanocytic lesions. A pre-trained model from ImageNet Large Scale Visual Recognition Challenge (ILSVRC) 2012 was utilized. The model consists of 5 convolutional layers. Kawahara et al. [259] presented an AlexNet based fully convolutional neural network for multiple scales feature computation. The approach excluded a pre-trained CNN. A classification accuracy of 81.8% was reported [259]. Andre et al. [39] utilized the CNN GoogleNet inception-V3 architecture pre-trained on ILSVRC. A wide and diverse dataset of 129,450 skin lesions comprising of 2032 diseases was utilized. The internal features learned by CNN were examined using t-distributed stochastic neighbor embedding. The outputs of a CNN on a test set are a set of probabilities indicating the malignancy per image. Further, they are compared with a threshold to compute the performance measures [39].

A deep residual network of more than 50 layers was used for skin lesion classification in [5]. Residual network comprises of stacked layers consisting of convolutional layer, rectified linear unit and batch normalization layer. The 2015, ImageNet pre-trained dataset model was used for the initialization of the weights and deconvolutional layers were initialized using bilinear interpolation weights. The vanishing gradient problem and the degradation problem are encountered, as the number of layers increases in deep neural networks. The former is a difficulty arising in training the network leading to inappropriate parameter tuning and the latter deals with the difficulty in holding on the performance gains. Effective methods such as careful initialization [103], batch normalization [261], and residual learning techniques [262] have been developed to train the network with large number of layers. Additionally, a limited dataset contributes negatively to the generalization capability. Attempts have been made to increase the dataset by cropping

and rotating [263], major axis alignment and augmentation [264]. Diverse and a wide dataset of skin lesions can enhance the classifier generalization ability to differentiate the melanocytic lesions. The ISBI 2017 challenge, part 3 was addressed by using an ensemble of CNN's by Matsunaga et al. [265]. Optimization techniques such as RMSProp and AdaGrad were used for fine tuning of the CNNs. Currently, the deep learning field pertaining to dermoscopic image classification is an evolving field.

8.5. Decision trees

A decision tree develops classifiers by separating the information into more diminutive and uniform groups. A graphical representation of the decisions made, the events that may occur, and the outcomes associated with coalescences of decisions and events are depicted by the decision tree [266]. Visually Tuned Decision Tree (VTDT) is a decision tree predicated relegation system which sanctions the cessation-users to tune the trees manually. It illustrates that decision tree engender comprehensible rules to domain experts and sanction human experts to insert their domain erudition in planning the decision making models.

In computerized melanoma diagnosis system, decision trees are selected because of the cognition capability, interpretability and intuitiveness. Two approaches were utilized by Zhou et al. [267], in the first approach the feature vectors are stacked together and victualed into the decision tree and the final output is engendered by larger part voting of the member decision trees. This methodology had data gap quandary due to the heterogeneous data. The second approach used geometric and color metric features and due to homogeneity of the data, the data gap quandary was addressed. Although, the second approach performed better it was not straightforward approach [267]. The involution of decision tree depends on the nodes or number of rules extracted from the tree. The most popular decision tree approach is the C4.5 and CART (Classification and Regression Tress). CART are machine learning methods for constructing prognostication models from the data. The data space is partitioned and followed by fitting the simple presage model with each partition graphically representing a decision tree [268]. Wiltgen et al. [269] used CART wherein the image square components were part into disjunctive hubs and described by pertinent subset of features resulting in a sensitivity and specificity of 92.09% and 92.75% respectively. In many relegation quandaries though decision trees are facile to understand it is hard to find optimal threshold since data set representation is perpetual, consequently it gives a poor performance when compared to other classifiers [256]. Decision tree classifiers perform well on training data but for unseen data they do not generalize well. The C4.5 algorithm averts over fitting by distinguishing sub trees that contribute little to predictive exactness and superseding each by a leaf.

8.6. Logistic regression

Logistic regression is a factual strategy for breaking down a dataset in which there are one or more autonomous variables that decide a result. It constructs a disuniting hyper-plane between the two data sets. Logistic regression give a functional form f and parameter vector α to express P (y|x) as illustrated in Eq. (7)

$$P(y|x) = f(x, \alpha) \tag{7}$$

The parameter alpha is tenacious by the minimum likelihood function. Logistic regression is a parametric method because the contribution of parameters can be interpreted. Logistic regression can be utilized for PSL relegation assignments since the input variables are obtained from an image segmentation algorithm and not specifically from human interpretable visual features. Dreiseitl et al. [270] build a logistic regression model utilizing a subset of consequential covariates. The risk of developing melanoma was soothsaid utilizing the model developed from a questionnaire predicated on patient self-assessment of symptoms. Logistic regression odds ratio was utilized in [271] for diagnosis of thinner melanomas with veneration to dermatologists assessment. A logistic regression model that incorporates perfect covariates is called fundamental impacts model.

Logistic regression model figures the class participation likelihood for one of the two classifications of data sets. It sanctions interpretation of the results as probabilities and variable select capability. Albeit, it provides higher flexibility due nonlinear covariates it carries a higher risk for model over-fitting. Dreiseitl et al. [256] concluded that logistic regression performance level is same as ANN and SVM classifiers. Three variants of logistic regression namely the multinomial logistic regression, simple logistic regression and proportional odds model (POM) is used in [272], for classification of melanoma lesions. Multinomial logistic regression comprises of several binary logistic regression models. Simple logistic regression creates multinomial logistic regression using Logitboost. POM habituates the ordinal case with the standard logistic regression.

8.7. Ensemble classifiers

Ensemble classification approaches involve the integration of homogenous or heterogeneous classification algorithms to provide robust and accurate classification results in comparison to single classifier approach. Depending on the classifier output, the classification strategy varies. Manipulation of the training data is through bagging [273] and boosting [200,76,274]. Several ensemble methods have been used for the classification of skin lesions. Adaptive Boosting (AdaBoost) is one of the variants of the basic boosting technique. The main idea is to add weak classifiers until a minimum target error is reached. AdaBoost mainly concentrates on the samples that are difficult to classify. If a sample is not correctly classified by the initial component classifier, it is passed on to the subsequent stage for further classification. Each of the training samples are assigned weights, the weight determines the probability of a training sample to be selected for classification. In [275], classification using AdaBoost classifier built using decision trees outperformed SVM classification. In [276], a hybrid AdaBoost classifier is proposed considering SVM as a base classifier which is consequently trained using gentle AdaBoost. The hybrid approach indicated better results in comparison to the stand alone gentle AdaBoost approach.

Alcon et al. [149], built a meta AdaBoost classifier using decision trees, Logistic Model Trees and Bayesian Networks for classification of benign and malignant lesions. The features selected for classification were rotation and scale invariant. The classifier reported an average accuracy of 68% [149]. Xie et al. [278], designed a neural network meta-ensemble model for classification of malignant lesions. Three results from three ensemble models were combined to yield the final classification. Each of the three ensemble models varied in number of hidden layers, types of structures (back propagation network/Fuzzy Neural Network), and network structures (Same/different) [278]. A neural network ensemble model provides better stability and generalization ability, in comparison to a single network, thereby achieving more reliable classification. Abbas et al. [279], designed an ensemble classifier Learn++ using neural networks for recognizing 12 categories of skin lesions. The algorithm randomly selects the training data and a query image is labelled based on majority voting scheme.

8.8. Bayesian network

The Naive Bayes (NB) is a simple classifier that performs quiet well by computing the probabilities of the features extracted for skin lesions [280]. Garnavi et al. [167] adopted Hidden Naive Bayes (HNB) for a set of wavelet features achieving a classification accuracy of 86.27%. The features need to be independent in nature. NB classifier shows a faster convergence rate, if there exists conditional independence. However, it does not learn the relationship between the feature sets.

8.9. Other classifiers

Linear classifiers with threshold values were used for building 3 classification models (layered model and 2 flat models) for classification of four different skin lesions (Melanoma, Nevus, Basal cell carcinoma, and Seborrheic keratosis) [281]. For the purpose of classification, comparison of the classifiers output with a threshold value was performed. The layered model outperformed the 2 flat models. Hidden Markov Model (HMM) are a set of stochastic automata consisting of finite number of states N. In [282], classification of melanoma lesions is performed using HMM. In the initial phase, the HMM is built for the individual classes and then these models are further used to determine the class of the input sequence. K-means algorithm is applied to the histograms of the diagnosed lesions, to develop prototypes of the classes. These sequences serve as input to the Baum-Welch algorithm to build the Markov models. The model achieved a classification accuracy of 77%. Kernel logistic Partial Least Squares (KL-PLS) is used in [283] for classification of benign and malignant skin lesions. KL-PLS is used for binary classification, the classifier spans a discriminant space and combines the kernel map with logistic regression.

Classification of melanocytic lesions using wavelet based tree structure is proposed in [284]. In the training phase, the ratio of average channel energy to the highest channel energy at the same level is used as a threshold for wavelet channel decomposition, producing tree like topologies of the known classes. In the testing phase, the test images are decomposed using the thresholds computed in the training phase to build tree structures. Further, Mahanalobis distance is used for classification. Arbitrary selection of threshold was the major limitation of the method [284]. An Adaptive Wavelet Transform (ADWAT) based tree structure classification is proposed in [285]. Several ratios of channel energies are used as a feature set followed by histogram statistical analysis to compute the threshold for creating a wavelet decomposition. The approach resulted in a true positive rate of 90%. An extension of the work [285] was performed in [286], wherein an extra class termed "suspicious" was included in the test phase. Incomplete tree structures were assigned to the suspicious class followed by analyzing their transillumination images.

Fuzzy logic based classifiers are considered useful if the selected features exhibit an overlapping distribution among classes. The extent or the probability of a sample belonging to a particular class is indicated by a membership function. The value of the membership function ranges from 0 to 1. The parameterized functions used for defining the membership functions are triangular, trapezoidal, Gaussian and Bell. In [286], Gaussian and bell membership functions are computed for the two classes (melanoma and dysplastic nevus) using the feature vector values. Consequently, the query image is assigned to the image class with a higher membership function value. It is observed that Bell profile based membership function proved to be effective with a true positive rate of 100%. Neuro-Fuzzy Classifiers combine the learning capability of neural networks with the reasoning capability of fuzzy systems. They are considered as universal approximations provided with the ability to use if-then rules. In [287], the images are tested using hierarchical neural network and consequently passed through a fuzzy logic inference module resulting in a sensitivity and specificity of 98% and 89% respectively. It is inferred from the study [287] that the efficacy of the neuro-fuzzy systems mainly depends on the feature extraction techniques. Adaptive Neuro Fuzzy Inference System (ANFIS) is a fuzzy Sugeno architecture that facilitates learning and adaption. The ANFIS architecture consists of five layers, the first and the fourth layer are the 2 adaptive layers. The second, third and fifth layers are the fixed layers. The training of ANFIS involves the tuning of the modifiable and premise parameters present in the first and fourth layers respectively [289]. Odeh used the gradient descent method in conjunction with the least squares method for training of the ANFIS architecture to classify melanoma lesions from other skin cancers [290]. Premaladha et al. [276], used fifteen features extracted from dermatological images as input to the ANFIS system utilizing a triangular membership function for classification of melanocytic lesions. Tasoulis et al. [292] proposed the Principal Direction Divisive Partitioning algorithm (PDDP) termed as dePDDP for classification of melanoma from dysplastic nevus. PDDP is a hierarchical clustering algorithm that utilizes information from the first singular vector of the principle component analysis to select the splitting clusters and determine the termination criterion. The dePDDP is a variant of the PDDP, which utilizes the global minimum of the density function from the first principal component as a criteria for splitting of clusters [292].

Extreme Learning Machine (ELM) is the learning algorithm for single hidden layer feed forward network. In ELM, the hidden layer parameters are randomly generated and thus do not require tuning, thereby leading to the prior establishment of the hidden nodes [293]. The tuning of the output weights is performed by regularized least squares method, which tends to be faster compared to the SVM quadratic programming problem, and gradient descent method of Back Propagation Network. For medical image classification, it is essential to perform feature learning prior to classification. However, ELM provides a shallow architecture in this regard. One possible solution to this could be deployment of ELM for multilayer perceptron [294]. Genetic algorithms are used in classification tasks to search among a space of potential solutions in order to find an optimal solution. Genetic algorithms can be used to train neural networks, to search rule sets. Genetic algorithms have garnered significant attention for classification mainly due to the following reasons. First, genetic algorithms can be used to train neural networks, search rule sets on discrete spaces. The learning system performance is determined by the fitness parameter unlike the back propagation method, thus making it a favorable choice in case where information is used as a performance measure. During the training phase, the fitness is evaluated for all the chromosome and the fittest chromosome is selected as the new weight. Classification of various skin lesions using ANN-GA achieved a classification ratio of 78.8% in [295].

9. Performance evaluation

Diagnosis is concerned with determining the prevailing flow condition of the patient and precisely distinguishing the current illness state. In analytic models, the objective is the exact arrangement of people into their actual disease state. In diagnostic models, the goal is the precise classification of individuals into their true disease state. In binary classification, it includes distinguishing of normal nevi from dysplastic nevi and melanoma or recognizing melanoma from prevalent nevi and dysplastic nevi. Multiclass classification involves correctly distinguishing three or more states. Several criteria may be acclimated to evaluate the performance of relegation algorithms. The two criteria for evaluation of presages include discrimination and calibration. Discrimination aims to rel-

egate individuals into categories, it is the facility to dissever those with or without disease. Discrimination is a definitive objective of symptomatic models.

Calibration is measure of how close the forecasts of a given model match the likelihood of transfer as given by expert. It refers to the acquiescent between examined end points and presages and concerns itself straightforwardly with the assessed probabilities or prescient values [291]. The disease prevalence is estimated by the positive and negative predictive values. Calibration can be assessed graphically, x-axis giving the prognostications, and the observed endpoint betokened on y-axis. Calibration is customarily near perfect at model development, and especially of interest at external validation. These aspects do not assess the competency to settle on preferable choices with a model over without. The Hosmer-Lemeshow goodness of fit test is the most well-known measure of calibration [291]. It provides a P-value for distinctions between observed and prognosticated endpoints per group of patients and also denotes the direction of any miscalibration. Decision threshold cut-off gives the evaluation of relegation for a soothsaid risk to define a low and high risk group. The balance between the advantage of genuine positive assignment and the harm of duplicitous positive transfer defines the ideal threshold [288].

Confusion matrix defines relegation quandaries with the quantities of cases effectively and mistakenly relegated for each class the matrix gives a detailed breakdown of correct and erroneous relegations for each class. The rows and columns of the matrix correspond to ground truth labels and prognostication respectively. False positives (FP) are cases soothsaid as positive from the negative class. False negatives (FN) are cases anticipated as negative whose genuine class is certain. True positives (TP) betokens cases anticipated as relating to the positive class and True negatives (TN) assign cases accurately soothsaid as belonging to the negative class. Sensitivity and specificity are the most commonly used performance evaluation parameters. Sensitivity is the competency of a test to accurately distinguish those with the disease. It is furthermore kenned as recall. Specificity is the capacity of the test to effectively distinguish those without the ailment. The sum of sensitivity and specificity ignores the relative weight of true positives and erroneous positives [260]. Accuracy simply measures how often the classifier makes the correct prognostication. It is the ratio between the number of correct presages and the total number of prognostications.

A performance measure in case of range of scores is Receiver Operating Characteristic curve (ROC). The Area Under the Curve (AUC) is kenned as c-statistic, it can range from no predictability to idealize discrimination. The ROC curve may be subsidiary when the specificity or sensitivity for a melanoma screening test must be above a threshold value for clinical use. The optimal threshold ought to be a component of the relative expenses of misclassifying diseased and non-diseased individuals [250]. Error evaluates a classifier by its percentage of erroneous presages. It is complement of accuracy. If the output of the classifier is a numeric probability in lieu of a class label of 0 or 1 then, logarithmic loss can be utilized which gives finer details of the classifier. It incorporates this conception of probabilistic confidence [246]. Precision (P) is a quantification which evaluates the likelihood that a positive expectation is right.

The classification model is built on the training set and is applied to the test set. The training/testing ratio used by Ercal et al. [243] was 20/80, 40/60, 60/40. The conception is that more training data gives better generalization and because it makes the relegation model better, whereas an immensely colossal test data makes the error estimate more precise. The available finite set of data can be partioned to training and test sets by Hold-out, cross validation and bootstrapping method. The hold-out method desultorily partitions the data into training multi-set and test set. In k-fold cross validation the preparation set is randomly separated into k-disjoint arrangements of equivalent size and every part has generally the same class appropriation. The classifier is trained k-times with various set utilized every time as a test set [291]. Leave one out is a unique instance of cross validation by utilizing the total number of samples in the training set as the value of k. If k designates the total number of samples, the leave one out method uses k-1 samples for training and one sample for testing. Leave one out method is computationally extravagant and does not ensure the same class distribution in training and test data. Balanced training and test ratios can be visually perceived as the vicissitude in penalty function, wherein the majority class pattern occurs less often. For two class quandaries in order to balance the unbalanced data, a balanced training set can be built by desultorily selecting the desired number of minority class instances simultaneously integrating equal number of desultorily selected majority class instances. Similarly, a balanced set not the same as training set can be built to test the classifier. For multi-class quandaries, each class can be represented approximately by equal proportions of training and test data sets. Rather than relying on a single decision scheme for evaluating the performance of the classifiers, individual evaluation parameters should be combined to derive a consensus decision of the classifier performance. The Table 3 gives the classifier evaluation parameters reported in literature. The Table 4 outline details of the state of art approaches used for dermoscopy image analysis.

Table 3
Classifier evaluation parameters.

Evaluation Parameters	Formulae
Accuracy	$\frac{TN+TP}{FN+FP+TN+TP}$
Error rate	$\frac{FN+FP}{FN+FP+TN+TP}$ (1- Accuracy)
Sensitivity Or Recall (R)	$\frac{TP}{FN+TP}$
Specificity	$\frac{TN}{FP+TN}$
Precision (P)	$\frac{TP}{TP+FP}$
Diagnostic Accuracy	$\frac{TP}{FN+FP+TP}$
LR_+(Likelihood ratio for positive test)	Sensitivity/(1- Specificity)
LR- Likelihood ratio for negative test)	(1-Sensitivity)/Specificity
Diagnostic Odds Ratio	$\frac{TP/FN}{FP/TN}$
Positive predictive value	$\frac{TP}{TP+FP} * 100\%$
Negative predictive value	$\frac{TN}{TN+FN} * 100\%$
F- measure	$\frac{\left(\beta^2+1\right)*P*R}{\beta^2+P+R}$ β is equal to 1
Index of suspicion	$\frac{TP+FP}{TP+FN} * 100$
Logarithmic loss	$\left(-\frac{1}{N}\right)\sum_{i=1}^{N} y_i log p_i + (1-y_i)\log(1-p_i)$ p_i probability of ith data point belongs to class 1 $y_i$true label either 0 or 1

10. Discussion and conclusion

Diagnosis of cutaneous melanoma has been a dynamic research area throughout the years, as far as diagnostic calculations as well as skin imaging technologies, which include support by dermoscopy and computer aided diagnostic are concerned [6,143]. In the published literature, the precision accomplished by current dermoscopy CAD framework for melanoma analysis is similar to the exactness accomplished by the dermatologist. To develop and validate sophisticated algorithms and systems supporting new imaging techniques, it demands a lot of research and innovative system development. A major drawback to dermoscopy is that,

Table 4
Summary state of art approaches.

Year	Segmentation method	Feature Extraction	Classification	SE	SP	Acc.	PT	Comments	Ref.
2017	Fully Convolutional Residual Network	–	Deep Residual Network	0.547	0.931	0.855	0.84s	Residual learning is used to avoid the limited training data problem	[103]
2016	Geodesic active contour	Asymmetry, Border Irregularity, Color, Differential Structures	TDS is calculated	0.912	0.958	0.94	-n	Pigment Network, Blue-white veil and Geometrical Properties were extracted for Differential Structures.	[170]
2017	Ant Colony Based Segmentation	Shape, Color and Texture Features	KNN, ANN	-n	-n	85.22% for KNN 93.60% for ANN	-n	Relief algorithm was used for feature selection. Twelve features were selected	[110]
2013	Thresholding +Improved Dynamic Programming	Asymmetry, Border Irregularity, Color, Differential Structures	SVM	88.2%	91.3%	-n	5.49s	Sequential floating forward selection, CASH features can be accommodated for developing a complete diagnostic system	[63]
2016	Chan-Vese	Asymmetry,Border, Color, Texture	SVM	-n	-n	74.36%	4.48s	Classification accuracy for Nevus-Keratosis is 79.01%, Classification accuracy for Keratosis-Melanoma is 74.33%, Histogram Intersection–Kernel	[96]
2013	450 × 450 ROI is selected	Color Multi-scale Texture features	ML-SVM ML-KNN AdaBoost MC	89.2%	93.75%	-n	3.65s	The color-texture features agree with dermatologist perception	[175]
2015	–	High level Intuitive Features	LIBSVM	-n	-n	83.59%, 81.36%, 81.17%	-n	Three different values of accuracy was obtained for different values of β of optimization function	[93]
2015	Otsu thresholding +Active Contour using Sparse-Field level-set method	2-FFT(4) 2-DCT (4) Complexity (3) Color (64) Pigment network(5)+4 features	LibSVM	-n	-n	Benign = 96.3% Atypical = 95.7% Melanoma = 97.5%	-n	Comparison between one-level and two-level classifiers is performed Two level classifiers out performs one-level classifier.	[53]
2012	Global thresholding + adaptive histogram thresholding	23 were selected out of 35455	SVM+ RF+ LMT+ HNB classifiers	-n	-n	91.26% AUC = 0.937	-n	Gain Ratio Method was used for feature selection	[167]
2009	Threshold	Asymmetry, Border Color, Texture	Bayesian	94%	68%	86%	-n	Correlation based feature selection was used	[149]
2008	Clustering + Region Growing	Color, Symmetry, Border, texture	ANN	85.9%	86%	-n	3 to 5s	Internet based web server is developed	[151]
2008	Region Growing+ Region Merging based on color	Shape, Color, texture	SVM	93.3%	92.34%	-n	5 to 10s	CFS, Mutual information based feature selection (MIFS) and ReliefF feature Selection algorithm were used	[152]
2010	Normalized Cut	Border Irregularity	Discriminant Analysis	74.2%	72.6%	-n	-n	Centroid distance is powerful for characterizing the border irregularity	[169]
2004	Laplacian filter+ zero crossing algorithm	Geometry, colors textures and islands of color	KNN	98%	79%	-n	-n	PSL were acquired by four computerized analyzers (DB-Mips) situated in two distinctive dermatological units.	[99]
2005	-n	Lesions were excised and examined histologically	-n	-n	100%	90%	-n	A software was developed given a score for the lesion within a range of 1–10	[137]
2015	-n	Global+ local+ ABCD	Naive Bayes +Random forest	-n	-n	84.16%	-n	CFS subset evaluation	[250]
2016	Circular center of each PSL	Color+ texture	MV-SVM	94%	84%	93%	1.6s	Seven skin lesion patterns are classified	[247]

PT indicates Performance Time.
-n indicates Not Mentioned.
** Indicates not performed.

it is highly subjective and varies with experience. There arises a need of biopsy for differentiating dysplastic nevi from melanoma. Suspicious changes in nevi is not necessarily melanoma, consequently biopsying benign lesions can lead to expanded grimness to patients and increased expense to the healthcare systems [83,229]. There are critical obstructions to execution which needs to be addressed. Factors such as time, training, and experience needed to legitimately utilize numerous of the available and emerging technologies pose a significant barrier to the early diagnosis of melanoma.

Detection has remained a significant challenge particularly in small diameter lesions leading to sensitivity of 71% for melanomas of less than 6 mm [227]. However, most of the dermatologist believe that only lesions over 5 mm are considered as melanomas [196]. According to the literature [184], lesions with less than 6 mm diameter account for 11.4% to 38.2% of all melanomas. In some cases, Total Body Scan Equipment (TBSE) is developed for detection of skin lesions malignancy [164]. Although, the risk of overlooking a malignant lesion because of the failure to perform TBSE is 2.17% [196], it has a constraint of being tedious and relentless and costs can run as high as $500 per person. Although, an automated image analysis module and an application for tracking the time for the evolution of skin lesions was been developed, a complete decision support system has not been developed [214].

This review provides an overview of the current advancements in computerized analysis of PSLs using dermoscopic images. A thorough introduction comprising of the domain and technical aspects is provided. Existing and emerging computational methods addressing automated segmentation and feature extraction were presented. Additionally, skin lesion classification methods based on conventional and newly developed state of art approaches have been included. The present scenario indicates that histopathological diagnosis continues to remain a gold standard for skin lesion diagnosis. However, histopathological diagnosis can be replaced in the near future by CAD systems that address the issues mentioned below.

- Skin lesion elevation and evolution features may be explored. In order to obtain comprehensive analysis of the lesion, multiple images of the same lesion covering various aspects should be acquired, which can lead to classification according to level of malignancy. This requires a publicly available annotated dataset with essential diagnostic information in this regard. Such kind of dataset is anticipated in the near future, and to the best of knowledge, there are no publicly available databases with annotations describing elevation and evolution features.
- Image segmentation determines the quality of the final analysis, decorrelated color spaces can be explored in order to examine the impact of these color spaces in border detection. Performance metrics such as Jaccard index and dice coefficients can also be incorporated as evaluation parameters.
- A fusion of geometrical and dermoscopic features would aid in building a more robust CAD system for PSLs.
- It has been observed that only few studies report the optimal feature selection procedures necessary to reduce the redundancy and intricacy of the classifiers. A very important task is selection of potential features without the loss of information. Different feature selection models can be explored to determine the relevance of the features with respect to the skin lesion type.

The potential benefits of the computerized solution to PSL detection is tremendous. However, accurate detection also seems to be a tedious task which necessarily increases the demand for reliable automated detection process that can be adopted routinely in the diagnostic process by expert and non-expert clinicians. It is inferred from the review that, CAD systems developed for PSLs have indicated good performances in experimental settings. A computer aided diagnostic system should be subjected to rigorous validation tests before it is accepted in a real world clinical setting and deployed as a smart phone application.

Acknowledgements

The authors express their gratitude to Prof. Tanweer, REVA University Bangalore, for his extensive support and contribution in carrying out this research. This work was supported by Manipal University Dr. T.M.A Pai Research Scholarship under Research Registration No. 160900105-2016.

References

[1] Cancer Facts & Figs. 2016. https://www.cancer.org/research/cancer-facts statistics/all-cancer-facts-figures/cancer-facts-figures-2016. html (Accessed: 10 August 2016).
[2] R. Lag, D. Harkins, M. Krapcho, A. Mariotto, B.A. Miller, E.J. Feuer, L. Clegg, M.P. Eisner, M.J. Horner, N. Howlader, M. Hayat, Seer Cancer Statistics Review, National Cancer Institute, Bethesda, 1975, pp. 1975–2012.
[3] R.L. Siegel, K.D. Miller, A. Jemal, Cancer statistics 2016, CA : A Cancer J. Clini. 66 (1) (2016) 7–30.
[4] Michael A. Davies, Ping Liu, Susan McIntyre, Kevin B. Kim, Nicholas Papadopoulos, Wen-Jen Hwu, Patrick Hwu, Agop Bedikian, A Prognostic factors for survival in melanoma patients with brain metastases, Cancer 117 (2011) 1687–1696.
[5] A. Blum, R. Hofmann-Wellenhof, H. Luedtke, U. Ellwanger, A. Steins, S. Roehm, C. Garbe, H.P. Soyer, Value of the clinical history for different users of dermoscopy compared with results of digital image analysis, J. Eur. Acad. Dermatol. Venereol. 18 (6) (2004) 665–669.
[6] C. Herman, Emerging technologies for the detection of melanoma: achieving better outcomes Clinical, Cosmet. Invest. Dermatol. 5 (2012) 195–212.
[7] Mercedes Filho, Joao Manuel, R.S. Tavares, A Review of quantification and classification of PSL from handheld to dedicated devices, J. Med. Syst. 39 (11) (2015) 1–12.
[8] Ammara Masood, Adel Ali Al-Jumaily, Computer aided diagnostic support system for skin cancer: a review of techniques and algorithms, Int. J. Biomed. Imaging (2013), 323268.
[9] Alfonso Baldi, Marco Quartulli, Raffaele Murace, Emanuele Dragonetti, Mario Manganaro, Oscar Guerra, Stefano Bizzi, Automated dermoscopy image analysis of pigmented skin lesions, Cancers 2 (2) (2010) 262–273.
[10] D. Gutman, N.C. Codella, E. Celebi, B. Helba, M. Marchetti, N. Mishra, A. Halpern, Skin Lesion Analysis Toward Melanoma Detection: A Challenge at the International Symposium on Biomedical Imaging (ISBI) 2016, hosted by the International Skin Imaging Collaboration (ISIC), 2016 (arXiv preprint arXiv:1605.01397).
[11] ISIC 2017: Skin Lesion Analysis Towards Melanoma Detection. https:// challenge.kitware.com/#challenge/n/ISIC_2017%3A_Skin_Lesion_Analysis_ Towards_Melanoma_Detection. [Online Accessed- 04 May 2017].
[12] Cancer Facts & Figs. 2017. https://www.cancer.org/research/cancer-facts-statistics/all-cancer-facts-figures/cancer-facts-figures-2017.html (Accessed: 11 June 2017).
[13] G.L. Beardmore, The epidemiology of malignant melanoma in Australia, Melanoma Skin Cancer (1972) 39–64.
[14] A. Uong, L.I. Zon, Melanocytes in development and cancer, J. Cell. Physiol. 222 (1) (2010) 38–41.
[15] Feng Ju, Nancy G Isern, Sarah D. Burton, Jian Zhi Hu, Studies of secondary melanoma on C57BL/6J mouse liver using 1H NMR metabolomics, Metabolites 3 (4) (2013) 1011–1035.
[16] D. Delgado, C. Butakoff, B.K. Ersboll, W.V. Stoecker, Independent histogram pursuit for segmentation of skin lesions, IEEE Trans. Biomed. Eng. 55 (1) (2008) 157–161.
[17] Ashfaq A. Marghoob, Josep Malvehy, Ralph P. Braun, An Atlas of Dermoscopy, 2nd edition, CRC Press, 2012.
[18] J. Jensen, Daniel Boni, E. Elewski, The ABCDEF rule combining the ABCDE rule and the ugly duckling sign in an effort to improve patient self-Screening examinations, J. Clin. Aesthetic Dermatol. 8 (2) (2015) 15.
[19] Wilhelm Stolz, Otto Braun-Falco, Peter Bilek, Michael Landthaler, Walter H.C. Burgdorf, Armand B. Cognetta, Color Atlas of Dermatoscopy, Wiley-Blackwell, 2002.
[20] S. Sacchidanand, A.S. Savitha, Nail & Its Disorders, JP Medical Ltd., 2013.
[21] R.M. Mackie, Cutaneous microscopy in vivo as an aid to preoperative assessment of pigmented skin lesions of the skin, Br. J. Plast. Surg. 25 (1972) 123–129.
[22] R. Johr, H.P. Soyer, G. Argenziano, R. Hofmann wellenhof, M. Scalvenzi, Dermoscopy: The Essentials, 2nd edn, Elsevier, Canada, 2017.
[23] Omar Noor, Anjali Nanda, Babar K. Rao, A dermoscopy survey to assess who is using it and why it is or is not being used, Int. J. Dermatol. 48 (9) (2009) 951–952.

[24] Anthony F. Jerant, Jennifer T. Johnson, C. Sheridan, Timothy J. Caffrey, Early detection and treatment of skin cancer, Am. Fam. Physician 62 (2) (2000) 357–368.
[25] Esther Erdei, Salina M. Torres, A new understanding in the epidemiology of melanoma, Expert Rev. Anticancer Ther. 10 (11) (2010) 1811–1823.
[26] H. Lorentzen, K. Weismann, C.S. Petersen, F.G. Larsen, L. Secher, V. Skodt, Clinical and dermatoscopic diagnosis of malignant melanoma, Acta Derm. Venereol. 79 (1999) 301–304.
[27] J.G. Fujimoto, C. Pitris, S.A. Boppart, M.E. Brezinski, Optical coherence tomography: an emerging technology for biomedical imaging and optical biopsy, Neoplasia 2 (1) (2000) 9–25.
[28] Gerger Armin, Silvia Koller, Thomas Kern, Cesare Massone, Karin Steiger, Erika Richtig, Helmut Kerl, Josef Smolle, Diagnostic applicability of in vivo confocal laser scanning microscopy in melanocytic skin tumors, J. Invest. Dermatol. 124 (3) (2005) 493–498.
[29] G. Pellacani, M. Vinceti, S. Bassoli, R. Braun, S. Gonzalez, P. Guitera, C. Longo, A.A. Marghoob, S.W. Menzies, S. Puig, A. Scope, Reflectance confocal microscopy and features of melanocytic lesions: an internet-based study of the reproducibility of terminology, Arch. Dermatol. 145 (10) (2009) 1137–1143.
[30] Pascale Guitera, Scott W. Menzies, Caterina Longo, Anna M. Cesinaro, Richard A. Scolyer, Giovanni Pellacani, In vivo confocal microscopy for diagnosis of melanoma and basal cell carcinoma using a two-step method: analysis of 710 consecutive clinically equivocal cases, J. Invest. Dermatol. 132 (10) (2012) 2386–2394.
[31] J.G. Fujimoto, Optical coherence tomography for ultrahigh resolution in vivo imaging, Nat. Biotechnol. 21 (11) (2003) 1361–1367.
[32] DermNet New Zealand. http://www.dermnetnz.org/ (Accessed: 11 June 2017).
[33] Gabriel Salerni, Cristina Carrera, Louise Lovatto, Joan Anton Puig-Butille, Celia Badenas, Estel Plana, Susana Puig, Josep Malvehy, Benefits of total body photography and digital dermatoscopy in the early diagnosis of melanoma in patients at high risk for melanoma, J. Am. Acad. Dermatol. 67 (1) (2012) 17–27.
[34] M. Elbaum, A.W. Kopf, H.S. Rabinovitz, R.G. Langley, H. Kamino, M.C. Mihm, A.J. Sober, G.L. Peck, A. Bogdan, D. Gutkowicz-Krusin, M. Greenebaum, Automatic differentiation of melanoma from melanocytic nevi with multispectral digital dermoscopy: a feasibility study, J. Am. Acad. Dermatol. 44 (2) (2001) 207–218.
[35] L. Serrone, F.M. Solivetti, M.F. Thorel, L. Eibenschutz, P. Donati, C. Catricala, High frequency ultrasound in the preoperative staging of primary melanoma: a statistical analysis, Melanoma Res. 12 (3) (2002) 287–290.
[36] Ichiro Ono, Fumio Kaneko, Magnetic resonance imaging for diagnosing skin tumors, Clin. Dermatol. 13 (4) (1995) 393–399.
[37] T. Nagaoka, Recent advances in diagnostic technologies for melanoma, Adv. Biomed. Eng. 5 (2016) 111–117.
[38] G. Argenziano, H.P. Soyer, S. Chimenti, R. Talamini, R. Corona, F. Sera, M. Binder, L. Cerroni, G. De Rosa, G. Ferrara, R. Hofmann-Wellenhof, Dermoscopy of pigmented skin lesions: results of a consensus meeting via the Internet, J. Am. Acad. Dermatol. 48 (5) (2003) 679–693.
[39] A. Esteva, B. Kuprel, R.A. Novoa, J. Ko, S.M. Swetter, H.M. Blau, S. Thrun, Dermatologist-level classification of skin cancer with deep neural networks, Nature 542 (7639) (2017) 115–118.
[40] E. Waltz, Computer Diagnoses Skin Cancers, 2017, January 25, from http://spectrum.ieee.org/the-human-os/biomedical/diagnostics/computer-diagnoses-skin-cancers (Accessed 08 June 2017).
[41] T. Mendonca, P.M. Ferreira, J.S. Marques, A.R. Marcal, J. Rozeira, pH 2: A dermoscopic image database for research and benchmarking, 2013 35th Annual International Conference of the IEEE Engineering in Medicine and Biology Society (EMBC) (2013) 5437–5440.
[42] Dermoscopy Atlas (Accessed 04 May 2017) http://www.dermoscopyatlas.com/index.cfm.
[43] Dermnet. http://www.dermnet.com/ (Accessed 04 May 2017).
[44] Atlas of Dermatology (Accessed 04 May 2017) http://www.danderm-pdv.is.kkh.dk/atlas/index.html.
[45] G. Argenziano, H.P. Soyer, V. De Giorgio, et al., Interactive Atlas of Dermoscopy (book and CD-ROM), EDRA Medical Publishing and New Media, 2000.
[46] Dermofit Image Library (Accessed 05 May 2017) https://licensing.eri.ed.ac.uk/i/software/dermofit-image-library.html.
[47] Dermquest. https://www.dermquest.com/results/?q=Malignant%20melanoma (Accessed 05 May 2017).
[48] DermIS, http://www.dermis.net/dermisroot/en/home/index.htm (Accessed 04 May 2017).
[49] Image and Vision Processing Lab, University of Waterloo. https://uwaterloo.ca/vision-image-processing-lab/research-demos/skin-cancer-detection, (Accessed 04 May 2017).
[50] Q. Abbas, I.F. Garcia, M. Emre Celebi, W. Ahmad, Q. Mushtaq, A perceptually oriented method for contrast enhancement and segmentation of dermoscopy images, Skin Res. Technol. 19 (1) (2013) 490–497.
[51] M. Emre Celebi, Hitoshi Iyatomi, Gerald Schaefer, Contrast enhancement in dermoscopy images by maximizing a histogram bimodality measure, Proc. Image Processing (ICIP), 2009 16th IEEE International Conference (2009) 2601–2604.
[52] Liu Zhao, Josiane Zerubia, Skin image illumination modeling and chromophore identification for melanoma diagnosis, Phys. Med. Biol. 60 (9) (2015) 3415.
[53] Abuzaghleh Omar, Buket D. Barkana, Miad Faezipour, Noninvasive real-time automated skin lesion analysis system for melanoma early detection and prevention, IEEE J. Ranslational Eng. Health Med. 3 (2015) 1–12.
[54] Paul Wighton, Tim K. Lee, M. Stella Atkins, Dermascopic hair disocclusion using inpainting, Med. Imag. Int. Soc. Opt. Photon. (2008) 691427.
[55] Tim Lee, Vincent Ng, Richard Gallagher, Andrew Coldman, David McLean, Dullrazor: a software approach to hair removal from images, Comput. Biol. Med. 27 (6) (1997) 533–543.
[56] Gunter Wyszecki, Walter Stanley Stiles, Color Science 8, Wiley, New York, 1982.
[57] Kimia Kiani, Ahmad R. Sharafat, E-shaver: an improved Dull Razor for digitally removing dark and light-colored hairs in dermoscopic images, Comput. Biol. Med. 41 (3) (2011) 139–145.
[58] M. D'Amico, M. Ferri, I. Stanganelli, Qualitative asymmetry measure for melanoma detection, Proc of the 2nd IEEE (2004), ISBI: 1155–1158.
[59] G. Fleming Matthew, Carsten Steger, Jun Zhang, Jianbo Gao, Armand B. Cognetta, Charles R. Dyer, Techniques for a structural analysis of dermatoscopic imagery, Comput. Med. Imaging Graph. 22 (5) (1998) 375–389.
[60] Feng-Ying Xie, Shi-Yin Qin, Zhi-Guo Jiang, Ru-Song Meng, PDE-based unsupervised repair of hair-occluded information in dermoscopy images of melanoma, Comput. Med. Imaging Graph. 33 (4) (2009) 275–282.
[61] Qaisar Abbas, M. Emre Celebi, Irene Fondon Garcia, Hair removal methods: a comparative study for dermoscopy images, Biomed. Signal Process. Control 6 (4) (2011) 395–404.
[62] S.M. Pizer, E.P. Amburn, J.D. Austin, R. Cromartie, A. Geselowitz, T. Greer, B. ter Haar Romeny, J.B. Zimmerman, K. Zuiderveld, Adaptive histogram equalization and its variations, Comput. Vision Graphics Image Process. 39 (3) (1987) 355–368.
[63] Q. Abbas, M. Emre Celebi, I.F. Garcia, W. Ahmad, Melanoma recognition framework based on expert definition of ABCD for dermoscopic images, Skin Res. Technol. 19 (1) (2013) e93–e102.
[64] A.A. Abbas, X. Guo, W.H. Tan, H.A. Jalab, Combined spline and B-spline for an improved automatic skin lesion segmentation in dermoscopic images using optimal color channel, J. Med. Syst. 38 (8) (2014) 80.
[65] D.D. Gómez, C. Butakoff, B.K. Ersboll, W. Stoecker, Independent histogram pursuit for segmentation of skin lesions, IEEE Trans. Biomed. Eng. 55 (1) (2008) 157–161.
[66] H.G. Adelmann, Butterworth equations for homomorphic filtering ofimages, Comput. Biol. Med. 28 (2) (1998) 169–181.
[67] S. Shan, W. Gao, B. Cao, D. Zhao, Illumination normalization for robust face recognition against varying lighting conditions, Proc. IEEE Int. Workshop Anal. Model. Faces Gesture (2003) 157–164.
[68] Josep Quintana, Rafael Garcia, Laszlo Neumann, A novel method for color correction in epiluminescence microscopy, Comput. Med. Imaging Graph. 35 (7) (2011) 646–652.
[69] M.E. Celebi, H. Iyatomi, G. Schaefer, W.V. Stoecker, Approximate lesion localization in dermoscopy images, Skin Res. Technol. 15 (3) (2009) 314–322.
[70] M. Messadi, A. Bessaid, A. Taleb-Ahmed, Extraction of specific parameters for skin tumour classification, J. Med. Eng. Technol. 33 (4) (2009) 288–295.
[71] L. Yin, R. Yang, M. Gabbouj, Y. Neuvo, Weighted median filters: a tutorial, IEEE Trans. Circuits Syst. II: Analog Digital Signal Process. 43 (3) (1996) 157–192.
[72] S.K. Meher, B. Singhawat, An improved recursive and adaptive median filter for high density impulse noise, AEU-Int. J. Electron. Commun. 68 (12) (2014) 1173–1179.
[73] Abdolreza Dehghani Tafti, Ehsan Mirsadeghi, A novel adaptive recursive median filter in image noise reduction based on using the entropy, Control System, Computing and Engineering (ICCSCE), 2012 IEEE International Conference (2012) 520–523.
[74] C.A. Barcelos, V.B. Pires, An automatic based nonlinear diffusion equations scheme for skin lesion segmentation, Appl. Math. Comput. 215 (1) (2009) 251–261.
[75] Catarina Barata, Jorge S. Marques, Jorge Rozeira, Detecting the pigment network in dermoscopy images: a directional approach, Proc Engineering in Medicine and Biology Society, EMBC, 2011 Annual International Conference of the IEEE (2011) 5120–5123.
[76] C. Barata, J.S. Marques, J. Rozeira, A system for the detection of pigment network in dermoscopy images using directional filters, IEEE Trans. Biomed. Eng. 59 (10) (2012) 2744–2754.
[77] S. Yang, B. Oh, S. Hahm, K.Y. Chung, B.U. Lee, Ridge and furrow pattern classification for acral lentiginous melanoma using dermoscopic images, Biomed. Signal Process. Control 32 (2017) 90–96.
[78] M.E. Celebi, G. Schaefer, H. Iyatomi, W.V. Stoecker, Lesion border detection in dermoscopy images, Comput. Med. Imaging Graph. 33 (2) (2008) 148–153.
[79] M.E. Celebi, H. Iyatomi, W.V. Stoecker, R.H. Moss, H.S. Rabinovitz, G. Argenziano, H.P. Soyer, Automatic detection of blue-white veil and related structures in dermoscopy images, Comput. Med. Imaging Graph. 32 (8) (2008) 670–677.
[80] Teresa Mendonca, Andre R.S. Marcal, Angela Vieira, Jacinto C. Jacinto Nascimento, Margarida Silveira, Jorge S. Marques, Jorge Rozeira, Comparison of segmentation methods for automatic diagnosis of dermoscopy images,

Proc Engineering in Medicine and Biology Society (EMBS) 29th Annual International Conference of the IEEE (2007) 6572–6575.
[81] M.E. Celebi, Q. Wen, H. Iyatomi, K. Shimizu, H. Zhou, G. Schaefer, A state-of-the-art survey on lesion border detection in dermoscopy images, in: Dermoscopy Image Analysis, 2015, pp. 97–129.
[82] R. Garnavi, M. Aldeen, M.E. Celebi, A. Bhuiyan, C. Dolianitis, G. Varigos, Automatic segmentation of dermoscopy images using histogram thresholding on optimal color channels, Int. J. Med. Med. Sci. 1 (2) (2010) 126–134.
[83] G. Sforza, G. Castellano, S.K. Arika, R.W. LeAnder, R.J. Stanley, W.V. Stoecker, J.R. Hagerty, Using adaptive thresholding and skewness correction to detect gray areas in melanoma in situ images, IEEE Trans. Instrum. Meas. 61 (7) (2012) 1839–1847.
[84] P.K. Sahoo, S.A. Soltani, A.K. Wong, A survey of thresholding techniques, Computer Vision Graphics Image Process. 41 (2) (1988) 233–260.
[85] M. Sezgin, Survey over image thresholding techniques and quantitative performance evaluation, J. Electron. Imag. 13 (1) (2004) 146–168.
[86] N. Otsu, A threshold selection method from gray-level histograms, Automatica 11 (285–296) (1979) 23–27.
[87] Jiang Guangyou, Kang Gewen, A threshold segmentation algorithm based on neighbourhood characteristics, Proc Electronic Measurement & Instruments (ICEMI) 10th International Conference (2011) 328–331.
[88] D. Mumford, J. Shah, Optimal approximations by piecewise smooth functions and associated variational problems, Commun. Pure Appl. Math 42 (1989) 577–685.
[89] M. Emre Celebi, H.A. Kingravi, H. Iyatomi, Y. Alp Aslandogan, W.V. Stoecker, R.H. Moss, J.M. Malters, J.M. Grichnik, A.A. Marghoob, H.S. Rabinovitz, S.W. Menzies, Border detection in dermoscopy images using statistical region merging, Skin Res. Technol. 14 (3) (2008) 347–353.
[90] Bo Peng, Lei Zhang, David Zhang, Automatic image segmentation by dynamic region merging, IEEE Trans. Image Process. 20 (12) (2011) 3592–3605.
[91] M. Sonka, V. Hlavac, R. Boyle, Image Processing, Analysis, and Machine Vision, 2 ed., PWS, 1998.
[92] M. Sadeghi, M. Razmara, T.K. Lee, M.S. Atkins, A novel method for detection of pigment network in dermoscopic images using graphs, Comput. Med. Imaging Graph. 35 (2) (2011) 137–143.
[93] R. Amelard, J. Glaister, A. Wong, D.A. Clausi, High-level intuitive features (HLIFs) for intuitive skin lesion description, IEEE Trans. Biomed. Eng. 62 (3) (2015) 820–831.
[94] M. Zortea, E. Flores, J. Scharcanski, A simple weighted thresholding method for the segmentation of pigmented skin lesions in macroscopic images, Pattern Recogn. 64 (2017) 92–104.
[95] A. Pennisi, D.D. Bloisi, D. Nardi, A.R. Giampetruzzi, C. Mondino, A. Facchiano, Skin lesion image segmentation using Delaunay Triangulation for melanoma detection, Comput. Med. Imaging Graph. 52 (2016) 89–103.
[96] R.B. Oliveira, N. Marranghello, A.S. Pereira, J.M.R. Tavares, A computational approach for detecting pigmented skin lesions in macroscopic images, Expert Syst. Appl. 61 (2016) 53–63.
[97] Q. Abbas, I.F. Garcia, M. Emre Celebi, W. Ahmad, Q. Mushtaq, Unified approach for lesion border detection based on mixture modeling and local entropy thresholding, Skin Res. Technol. 19 (3) (2013) 314–319.
[98] P. Schmid, Segmentation of digitized dermatoscopic images by two-dimensional color clustering, IEEE Trans. Med. Imaging 18 (2) (1999) 164–171.
[99] Marco Burroni, Rosamaria Corona, Giordana Dell'Eva, Francesco Sera, Riccardo Bono, Pietro Puddu, Roberto Perotti, Franco Nobile, Lucio Andreassi, Pietro Rubegni, Melanoma computer-aided diagnosis reliability and feasibility study, Clin. Cancer Res. 10 (6) (2004) 1881–1886.
[100] N.C. Yeo, K.H. Lee, Y.V. Venkatesh, S.H. Ong, Colour image segmentation using the self-organizing map and adaptive resonance theory, Image Vision Comput. 23 (12) (2005) 1060–1079.
[101] K. Simonyan, A. Zisserman, Very Deep Convolutional Networks for Large-scale Image Recognition, 2014 (arXiv preprint arXiv:1409.1556).
[102] J. Qi, M. Le, C. Li, P. Zhou, Global and Local Information Based Deep Network for Skin Lesion Segmentation, 2017 (arXiv preprint arXiv:1703.05467).
[103] L. Yu, H. Chen, Q. Dou, J. Qin, P.A. Heng, Automated melanoma recognition in dermoscopy images via very deep residual networks, IEEE Trans. Med. Imaging 36 (4) (2017) 994–1004.
[104] Y. Yuan, M. Chao, Y.C. Lo, Automatic skin lesion segmentation using deep fully convolutional networks with jaccard distance, IEEE Trans. Med. Imaging (2017), http://dx.doi.org/10.1109/tmi.2017.2695227.
[105] X. Yang, Z. Zeng, S.Y. Yeo, C. Tan, H.L. Tey, Y. Su, A Novel Multi-task Deep Learning Model for Skin Lesion Segmentation and Classification, 2017 (arXiv preprint arXiv:1703.01025).
[106] J. Liu, B. Zuo, The segmentation of skin cancer image based on genetic neural network, Proc of the WRI World Congress on Computer Science and Information Engineering (CSIE '09) (2009) 594–599.
[107] H. Zhou, G. Schaefer, A.H. Sadka, M.E. Celebi, Anisotropic mean shift based fuzzy c-means segmentation of dermoscopy images, IEEE J. Sel. Top. Signal Process. 3 (2009) 26–34.
[108] Q. Abbas, M.E. Celebi, I. Fondón García, M. Rashid, Lesion border detection in dermoscopy images using dynamic programming, Skin Res. Technol. 17 (1) (2011) 91–100.
[109] Q. Abbas, M.E. Celebi, I.F. García, Skin tumor area extraction using an improved dynamic programming approach, Skin Res. Technol. 18 (2) (2012) 133–142.
[110] Fekrache Dalila, Ameur Zohra, Kasmi Reda, Cherifi Hocine, Segmentation and classification of melanoma and benign skin lesions, Optik – Int. J. Light Electron Opt. (2017), http://dx.doi.org/10.1016/j.ijleo.2017.04.084.
[111] R. Kasmi, K. Mokrani, R.K. Rader, J.G. Cole, W.V. Stoecker, Biologically inspired skin lesion segmentation using a geodesic active contour technique, Skin Res. Technol. 22 (2) (2015) 208–222.
[112] P.G. Cavalcanti, J. Scharcanski, A coarse-to-fine approach for segmenting melanocytic skin lesions in standard camera images, Comput. Methods Programs Biomed. 112 (2013) 684–693.
[113] N. Tsumura, H. Haneishi, Y. Miyake, Independent-component analysis of skin color image, J. Opt. Soc. Am. A 16 (1999) 2169–2176.
[114] Orlando J. Tobias, Rui Seara, Image segmentation by histogram thresholding using fuzzy sets, IEEE Trans. Image Process. 11 (12) (2002) 1457–1465.
[115] A. Dalal, R.H. Moss, R.J. Stanley, W.V. Stoecker, K. Gupta, D.A. Calcara, J. Xu, B. Shrestha, R. Drugge, J.M. Malters, L.A. Perry, Concentric decile segmentation of white and hypopigmented areas in dermoscopy images of skin lesions allows discrimination of malignant melanoma, Comput. Med. Imaging Graph. 35 (2) (2011) 148–154.
[116] X.F. Diao, X.Y. Zhang, T.F. Wang, S.P. Chen, L.H. Li, Robust topology-adaptive snakes for medical ultrasonic image segmentation, Proc of Biomedical Engineering and Informatics (BMEI) 3rd International Conference 2 (2010) 527–530.
[117] Z. Ma, J.M. Tavares, Segmentation of skin lesions using level set method, in: International Symposium Computational Modeling of Objects Represented in Images, Springer International Publishing, 2014, pp. 228–233.
[118] M. Silveira, J.C. Nascimento, J.S. Marques, A.R.S. Marcal, T. Mendonca, S. Yamauchi, Comparison of segmentation methods for melanoma diagnosis in dermoscopy images, IEEE J. Sel. Top. Signal Process. 3 (2009) 35–45.
[119] M. Nourmohamadi, H. Pourghassem, Dermoscopy image segmentation using a modified level set algorithm, Comput. Intell. Commun. Networks (2012) 286–290.
[120] I. Fondón, Q. Abbas, M.E. Celebi, W. Ahmad, Q. Mushtaq, Software tool for contrast enhancement and segmentation of melanoma images based on human perception, IMAGE-A 3 (6) (2013) 45–48.
[121] F. Leobourgeois, F. Drira, D. Gaceb, Fast integral meanshift: application to color segmentation of document images, in: 12th International Conference on Document Analysis and Recognition, Washington, DC, 2013, pp. 52–56.
[122] A.R. Sadri, M. Zekri, S. Sadri, N. Gheissari, M. Mokhtari, F. Kolahdouzan, Segmentation of dermoscopy images using wavelet networks, IEEE Trans. Biomed. Eng. 60 (4) (2013) 1134–1141.
[123] S. Khalid, U. Jamil, K. Saleem, M.U. Akram, W. Manzoor, W. Ahmed, A. Sohail, Segmentation of skin lesion using Cohen-Daubechies-Feauveau biorthogonal wavelet, SpringerPlus 5 (1) (2016) 1603.
[124] Q. Qiu, V. Patel, R. Chellappa, Information-theoretic dictionary learning for image classification, IEEE Trans. Pattern Anal. Mach. Intell. 36 (11) (2014) 2173–2184.
[125] E.S. Flores, J. Scharcanski, Segmentation of pigmented melanocytic skin lesions based on learned dictionaries and normalized graph cuts, in: Proceedings of the 27th Conference on Graphics, Patterns and Images (SIBGRAPI 2014), IEEE, 2014 (pp. 33–682 40).
[126] E. Flores, J. Scharcanski, Segmentation of melanocytic skin lesions using feature learning and dictionaries, Expert Syst. Appl. 56 (2016) 300–309.
[127] X. Yuan, N. Situ, G. Zouridakis, A narrow band graph partitioning method for skin lesion segmentation, Pattern Recogn. 42 (6) (2009) 1017–1028.
[128] K.A. Norton, H. Iyatomi, M.E. Celebi, S. Ishizaki, M. Sawada, R. Suzaki, et al., Three-phase general border detection method for dermoscopy images using non-uniform illumination correction, Skin Res. Technol. 18 (3) (2012) 290–300.
[129] H. Castillejos, V. Ponomaryov, L. Nino-de-Rivera, V. Golikov, Wavelet transform fuzzy algorithms for dermoscopic image segmentation, Comput. Math. Methods Med. 2012 (2012), 578721.
[130] A. Wong, J. Scharcanski, P. Fieguth, Automatic skin lesion segmentation via iterative stochastic region merging, IEEE Trans. Inf. Technol. Biomed. 15 (6) (2011) 929–936.
[131] Z. Ma, J.M.R. Tavares, A novel approach to segment skin lesions in dermoscopic images based on a deformable model, IEEE J. Biomed. Health Inf. 20 (2) (2016) 615–623.
[132] M. Emre Celebi, Q. Wen, S. Hwang, H. Iyatomi, G. Schaefer, Lesion border detection in dermoscopy images using ensembles of thresholding methods, Skin Res. Technol. 19 (1) (2013) e252–e258.
[133] Q. Abbas, M.E. Celebi, I.F. Garcia, A novel perceptually-oriented approach for skin tumor segmentation, Int. J. Innov. Comput. Inf. Control 8 (3) (2012) 1837–1848.
[134] H. Zhou, X. Li, G. Schaefer, M.E. Celebi, P. Miller, Mean shift based gradient vector flow for image segmentation, Comput. Vision Image Understanding 117 (9) (2013) 1004–1016.
[135] G. Schaefer, M.I. Rajab, M.E. Celebi, H. Iyatomi, Colour and contrast enhancement for improved skin lesion segmentation, Comput. Med. Imaging Graph. 35 (2) (2011) 99–104.
[136] X. Yuan, N. Situ, G. Zouridakis, Automatic segmentation of skin lesion images using evolution strategies, Biomedical Signal Process. Control 3 (3) (2008) 220–228.
[137] M. Barzegari, H. Ghaninezhad, P. Mansoori, A. Taheri, Z.S. Naraghi, M. Asgari, Computer-aided dermoscopy for diagnosis of melanoma, BMC Dermatol. 5 (1) (2005) 8.

[138] H. Pehamberger, A. Steiner, K. Wolff, In vivo epiluminescence microscopy of pigmented skin lesions. I. Pattern analysis of pigmented skin lesions, J. Am. Acad. Dermatol. 17 (4) (2016) 571–583.
[139] H. Johr Robert, Dermoscopy: alternative melanocytic algorithms the ABCD rule of dermatoscopy, Menzies scoring method, and 7-point checklist, Clin. Dermatol. 20 (3) (2002) 240–247.
[140] Nadia Smaoui, Souhir Bessassi, A developed system for melanoma diagnosis, Int. J. Comput. Vision Signal Process. 3 (1) (2013) 10–17.
[141] F. Nachbar, W. Stolz, T. Merkle, A.B. Cognetta, T. Vogt, M. Landthaler, et al., The ABCD rule of dermatoscopy: high prospective value in the diagnosis of doubtful melanocytic skin lesions, J. Am. Acad. Dermatol. 30 (4) (1994) 551–559.
[142] Yu-Ichi Ohta, Takeo Kanade, S. Toshiyuki, Color information for region segmentation, Comput. Graphics Image Process. 13 (3) (1980) 222–241.
[143] A. Karargyris, O. Karargyris, A. Pantelopoulos, DERMA/Care: an advanced image-processing mobile application for monitoring skin cancer, Proceedings IEEE 24th Int. Conf. Tools Artif. Intell. (ICTAI) (2012) 1–7.
[144] V. Ng, B. Fung, T. Lee, Determining the asymmetry of skin lesion with fuzzy borders, Comput. Biol. Med. 35 (2) (2005) 103–120.
[145] Ezgi Unlu, Bengu N. Akay, Cengizhan Erdem, Comparison of dermatoscopic diagnostic algorithms based on calculation: the ABCD rule of dermatoscopy, the seven-point checklist, the three-point checklist and the CASH algorithm in dermatoscopic evaluation of melanocytic lesions, J. Dermatol. 41 (7) (2014) 598–603.
[146] F.M. Walter, A.T. Prevost, J. Vasconcelos, P.N. Hall, N.P. Burrows, H.C. Morris, et al., Using the 7-point checklist as a diagnostic aid for pigmented skin lesions in general practice: a diagnostic validation study, Br. J. Gen. Pract. 63 (610) (2013) e345–e353.
[147] J.S. Henning, S.W. Dusza, S.Q. Wang, A.A. Marghoob, H.S. Rabinovitz, D. Polsky, A.W. Kopf, The CASH (color architecture, symmetry, and homogeneity) algorithm for dermoscopy, J. Am. Acad. Dermatol. 56 (1) (2007) 45–52.
[148] Y. Chang, R.J. Stanley, R.H. Moss, W. Van Stoecker, A systematic heuristic approach for feature selection for melanoma discrimination using clinical images, Skin Res. Technol. 11 (3) (2005) 165–178.
[149] J.F. Alcon, C. Ciuhu, W. Ten Kate, A. Heinrich, N. Uzunbajakava, G. Krekels, D. Siem, G. De Haan, Automatic imaging system with decision support for inspection of pigmented skin lesions and melanoma diagnosis, IEEE J. Sel. Top. Signal Process. 3 (1) (2009) 14–25.
[150] Md. Amran Hossen Bhuiyan, Ibrahim Azad, Md Kamal Uddin, Image processing for skin cancer features extraction, Int. J. Sci. Eng. Res. 4 (2) (2013) 1–6.
[151] H. Iyatomi, H. Oka, M.E. Celebi, M. Hashimoto, M. Hagiwara, M. Tanaka, K. Ogawa, An improved internet-based melanoma screening system with dermatologist-like tumor area extraction algorithm, Comput. Med. Imaging Graph. 32 (7) (2008) 566–579.
[152] M.E. Celebi, H.A. Kingravi, B. Uddin, H. Iyatomi, Y.A. Aslandogan, W.V. Stoecker, R.H. Moss, A methodological approach to the classification of dermoscopy images, Comput. Med. Imaging Graph. 31 (6) (2007) 362–373.
[153] P.G. Cavalcanti, J. Scharcanski, Automated prescreening of pigmented skin lesions using standard cameras, Comput. Med. Imag. Graphics 35 (6) (2011) 481–491.
[154] M. Ramezani, A. Karimian, P. Moallem, Automatic detection of malignant melanoma using macroscopic images, J. Med. Signals Sens. 4 (4) (2014) 281–290.
[155] Catarina Barata, Margarida Ruela, Teresa Mendonça, Jorge S. Marques, A bag-of-features approach for the classification of melanomas in dermoscopy images: the role of color and texture descriptors, in: Computer Vision Techniques for the Diagnosis of Skin Cancer, Springer, Berlin, Heidelberg, 2014, pp. 49–69.
[156] R. White, D.S. Rigel, R. Friedman, Computer applications in the diagnosis and prognosis of malignant melanoma, Dermatol. Clin. 9 (4) (1992) 695–702.
[157] Ilias G. Maglogiannis, Elias P. Zafiropoulos, Characterization of digital medical images utilizing support vector machines, BMC Med. Inform. Decis. Mak. 4 (1) (2004) 1.
[158] Nikolay Metodiev Sirakov, Mutlu Mete, Nara Surendra Chakrader, Automatic boundary detection and symmetry calculation in dermoscopy images of skin lesions, Proc IEEE 2011 18th International Conference on Image Processing (ICIP) (2011) 1605–1608.
[159] A.R. Patel, V. Vejjabhinanta, K. Nouri, Clinical pearl: the evaluation of the surface area of small pigmented lesions, Int. J. Dermatol. 46 (8) (2007) 872–874.
[160] J. Jaworek-Korjakowska, R. Tadeusiewicz, Determination of border irregularity in dermoscopic color images of pigmented skin lesions, Engineering in Medicine and Biology Society (EMBC), 2014 36th Annual International Conference of the IEEE (2014) 6459–6462 (August).
[161] A. Bono, S. Tomatis, C. Bartoli, G. Tragni, G. Radaelli, A. Maurichi, R. Marchesini, The ABCD system of melanoma detection, Cancer 85 (1) (1999) 72–77.
[162] Benjamin S Aribisala, Ela Claridge, A border irregularity measure using a modified conditional entropy method as a malignant melanoma predictor, in: Image Analysis and Recognition, Springer, Berlin, Heidelberg, 2005, pp. 914–921.
[163] I.G. Maglogiannis, Emerging Artificial Intelligence Applications in Computer Engineering: Real Word AI Systems with Applications in eHealth, HCI, Information Retrieval and Pervasive Technologies, vol. 160, Ios Press, 2007.
[164] K. Korotkov, J. Quintana, S. Puig, J. Malvehy, R. Garcia, A new total body scanning system for automatic change detection in multiple pigmented skin lesions, IEEE Trans. Med. Imaging 34 (1) (2015) 317–338.
[165] M.F. Healsmith, J.F. Bourke, J.E. Osborne, R.A.C. Graham-Brown, An evaluation of the revised seven-point checklist for the early diagnosis of cutaneous melanoma, Br. J. Dermatol. 130 (1) (1994) 48–50.
[166] M. Ruela, C. Barata, J.S. Marques, J. Rozeira, A system for the detection of melanomas in dermoscopy images using shape and symmetry features, Comput. Methods Biomech. Biomed. Eng.: Imag. Visualiz. 5 (2) (2017) 127–137.
[167] R. Garnavi, M. Aldeen, J. Bailey, Computer-aided diagnosis of melanoma using border- and wavelet-based texture analysis, IEEE Trans. Inf. Technol. Biomed. 16 (6) (2012) 1239–1252.
[168] L. Ma, R.C. Staunton, Analysis of the contour structural irregularity of skin lesions using wavelet decomposition, Pattern Recognit 46 (1) (2013) 98–106.
[169] Y. Zhou, M. Smith, L. Smith, R. Warr, A new method describing border irregularity of pigmented lesions, Skin Res. Technol. 16 (1) (2010) 66–76.
[170] R. Kasmi, K. Mokrani, Classification of malignant melanoma and benign skin lesions: implementation of automatic ABCD rule, IET Image Proc. 10 (6) (2016) 448–455.
[171] I. Maglogiannis, K.K. Delibasis, Enhancing classification accuracy utilizing globules and dots features in digital dermoscopy, Comput. Methods Programs Biomed. 118 (2) (2015) 124–133.
[172] C. Barata, M. Ruela, M. Francisco, T. Mendonca, J.S. Marques, Two systems for the detection of melanomas in dermoscopy images using texture and color features, IEEE Syst. J. 8 (3) (2013) 965–979.
[173] Helen M. Shaw, William H. McCarthy, Small-diameter malignant melanoma: a common diagnosis in New South Wales, Australia, J. Am. Acad. Dermatol. 27 (5) (1992) 679–682.
[174] L. Ballerini, R.B. Fisher, B. Aldridge, J. Rees, A color and texture based hierarchical K-NN approach to the classification of non-melanoma skin lesions, in: Color Medical Image Analysis, Springer, Netherlands, 2013 (pp. 63–86).
[175] Q. Abbas, M.E. Celebi, C. Serrano, I. Fondon Garcıa, G. Ma, Pattern classification of dermoscopy images: a perceptually uniform model, Pattern Recognit 46 (1) (2013) 86–97.
[176] J.L.G. Arroyo, B.G. Zapirain, Detection of pigment network in dermoscopy images using supervised machine learning and structural analysis, Comput. Biol. Med. 44 (2014) 144–157.
[177] M.M. Rahman, P. Bhattacharya, B.C. Desai, A multiple expert-based melanoma recognition system for dermoscopic images of pigmented skin lesions, in: International Conference on Bioinformatics and Bioengineering, Athens, October 8–10, IEEE, 2008, pp. 1–6.
[178] I. Maglogiannis, C.N. Doukas, Overview of advanced computer vision systems for skin lesions characterization, IEEE Trans. Inf. Technol. Biomed. 13 (5) (2009) 721–773.
[179] P. Wighton, T.K. Lee, H. Lui, D.I. McLean, M.S. Atkins, Generalizing common tasks in automated skin lesion diagnosis, IEEE Trans. Inf. Technol. Biomed. 15 (4) (2011) 622–629.
[180] H. Iyatomi, K.A. Norton, M.E. Celebi, G. Schaefer, M. Tanaka, K. Ogawa, Classification of melanocytic skin lesions from non-melanocytic lesions, in: Engineering in Medicine and Biology Society (EMBC), 2010 Annual International Conference of the IEEE, IEEE., 2010, August (pp. 5407–5410).
[181] Y. Faziloglu, R.J. Stanley, R.H. Moss, W.V. Stoecker, R.P. McLean, Colour histogram analysis for melanoma discrimination in clinical images, Skin Res. Technol. 9 (2003) 147–155.
[182] F. Xie, Y. Wu, Z. Jiang, R. Meng, Dermoscopy image processing for Chinese, in: Computer Vision Techniques for the Diagnosis of Skin Cancer, Springer, Berlin, Heidelberg, 2014 (pp. 109–137).
[183] S. Seidenari, G. Pellacani, C. Grana, Computer description of colours in dermoscopic melanocytic lesion images reproducing clinical assessment, Br. J. Dermatol. 149 (3) (2003) 523–529.
[184] Grażyna Kamińska-Winciorek, Waldemar Placek, The most common mistakes on dermatoscopy of melanocytic lesions, Adv. Dermatol. Allergol./Postępy Dermatologii i Alergologii 32 (2015) 33.
[185] K. Mollersen, M. Zortea, K. Hindberg, T.R. Schopf, S.O. Skrøvseth, F. Godtliebsen, Improved skin lesion diagnostics for general practice by computer-aided diagnostics, in: M.E. Celebi, T. Mendonca, J.S. Marques (Eds.), Dermoscopy Image Analysis, CRC Press, Boca Raton, 2015, pp. 247–292.
[186] M. Abedini, Q. Chen, N.C.F. Codella, R. Garnavi, X. Sun, Accurate and scalable system for automatic detection of malignant melanoma, in: M.E. Celebi, T. Mendonca, J.S. Marques (Eds.), Dermoscopy Image Analysis, CRC Press, Boca Raton, 2015, pp. 293–343.
[187] H. Iyatomi, H. Oka, M.E. Celebi, K. Ogawa, G. Argenziano, H.P. Soyer, H. Koga, T. Saida, K. Ohara, M. Tanaka, Computer based classification of dermoscopy images of melanocytic lesions on acral volar skin, J Investig Dermatol 128 (8) (2008) 2049–2054.
[188] M.E. Celebi, H. Iyatomi, W.V. Stoecker, R.H. Moss, H.S. Rabinovitz, G. Argenziano, H.P. Soyer, Automatic detection of bluewhite veil and related structures in dermoscopy images, Comput. Med. Imaging Graph. 32 (8) (2008) 670–677.
[189] M.S. Lew, Principles of Visual Information Retrieval, Springer Science & Business Media, 2013.

[190] R. Haralick, K. Shanmugan, I. Dinstain, Textural features for image classification, IEEE Trans. Syst. Man Cybern. 3 (6) (1973) 610–622.
[191] L. Andreassi, R. Perotti, P. Rubegni, M. Burroni, G. Cevenini, M. Biagioli, P. Taddeucci, G. Dell'Eva, P. Barbini, Digital dermoscopy analysis for the differentiation of atypical nevi and early melanoma: a new quantitative semiology, Arch. Dermatol. 135 (12) (1999) 1459–1465.
[192] N. Dala, B. Triggs, Histograms of oriented gradients for human detection, Proc of the IEEE Computer Society Conference on Computer Vision and Pattern Recognition (2005) 886–893.
[193] P. Mohanaiah, P. Sathyanarayana, I. GuruKumar, Image texture feature extraction using GLCM approach, Int. J. Sci. Res. Publ. 3 (5) (2016) 1.
[194] Mariam A. Sheha, Mai S. Mabrouk, Amr Sharawy, Automatic detection of melanoma skin cancer using texture analysis, Int. J. Comput. Appl. 42 (20) (2012) 22–26.
[195] Fritz Albregtsen, Statistical texture measures computed from gray level co-occurrence matrices, in: Image Processing Laboratory, Department of informatics, university of Oslo, 2008, pp. 1–14.
[196] A. Bono, E. Tolomio, S. Trincone, C. Bartoli, S. Tomatis, A. Carbone, M. Santinami, Micro-melanoma detection: a clinical study on 206 consecutive cases of pigmented skin lesions with a diameter ≤3mm, Br. J. Dermatol. 155 (3) (2006) 570–573.
[197] L. Ballerini, R.B. Fisher, B. Aldridge, J. Rees, Non-melanoma skin lesion classification using colour image data in a hierarchical K-NN classifier, Proc. Biomedical Imaging (ISBI), 9th IEEE International Symposium (2012) 358–361.
[198] L. Ballerini, X. Li, R.B. Fisher, B. Aldridge, J. Rees, Content-based image retrieval of skin lesions by evolutionary feature synthesis, in: Applications of Evolutionary Computation, Springer, Berlin, Heidelberg, 2010, pp. 312–319.
[199] B. Shrestha, J. Bishop, K. Kam, X. Chen, R.H. Moss, W.V. Stoecker, S. Umbaugh, R.J. Stanley, M.E. Celebi, A.A. Marghoob, G. Argenziano, Detection of atypical texture features in early malignant melanoma, Skin Res. Technol. 16 (1) (2010) 60–65.
[200] M. Rastgoo, R. Garcia, O. Morel, F. Marzani, Automatic differentiation of melanoma from dysplastic nevi, Comput. Med. Imaging Graph. 43 (2015) 44–52.
[201] T. Tanaka, S. Torii, I. Kabuta, K. Shimizu, M. Tanaka, Pattern classification of nevus with texture analysis, IEEE J. Trans. Electr. Electron. Eng. 3 (1) (2008) 143–150.
[202] C. Barata, M. Emre Celebi, J.S. Marques, Melanoma detection algorithm based on feature fusion, in: 37th Annual International Conference of the IEEE Engineering in Medicine and Biology Society, Milan, August 25–29, IEEE, 2015, pp. 2653–2656.
[203] N. Situ, X. Yuan, G. Zouridakis, Assisting main task learning by heterogeneous auxiliary tasks with applications to skin cancer screening, J. Mach. Learn. Res. 15 (2011) 688–697.
[204] M. Anantha, R.H. Moss, W.V. Stoecker, Detection of pigment network in dermatoscopy images using texture analysis, Comput. Med. Imaging Graph. 28 (5) (2004) 225–234.
[205] C. Barata, J.S. Marques, J. Rozeira, Evaluation of color based key points and features for the classification of melanomas using the bag-of-features model, in: International Symposium on Visual Computing, Springer, Berlin, Heidelberg, 2013, July (pp. 40–49).
[206] R.P. Braun, O. Gaide, M. Oliviero, A.W. Kopf, L.E. French, J.H. Saurat, H.S. Rabinovitz, The significance of multiple blue-grey dots (granularity) for the dermoscopic diagnosis of melanoma, Br. J. Dermatol. 157 (5) (2007) 907–913.
[207] W.V. Stoecker, M. Wronkiewiecz, R. Chowdhury, R.J. Stanley, J. Xu, A. Bangert, B. Shrestha, D.A. Calcara, H.S. Rabinovitz, M. Oliviero, F. Ahmed, Detection of granularity in dermoscopy images of malignant melanoma using color and texture features, Comput. Med. Imaging Graph. 35 (2) (2011) 144–147.
[208] A. Madooei, M.S. Drew, M. Sadeghi, M.S. Atkins, Automatic detection of blue-white veil by discrete colour matching in dermoscopy images, in: International Conference on Medical Image Computing and Computer-Assisted Intervention, Springer, Berlin, Heidelberg, 2013, September (pp. 453–460).
[209] W.V. Stoecker, K. Gupta, R.J. Stanley, R.H. Moss, B. Shrestha, Detection of asymmetric blotches (asymmetric structureless areas) in dermoscopy images of malignant melanoma using relative color, Skin Res. Technol. 11 (3) (2005) 179–184.
[210] G. Pellacani, C. Grana, R. Cucchiara, S. Seidenari, Automated extraction and description of dark areas in surface microscopy melanocytic lesion images, Dermatology 208 (1) (2004) 21–26.
[211] G. Fabbrocini, G. Betta, G. Di Leo, C. Liguori, A. Paolillo, A. Pietrosanto, P. Sommella, O. Rescigno, S. Cacciapuoti, F. Pastore, V. De Vita, Epiluminescence image processing for melanocytic skin lesion diagnosis based on 7-point check-list: a preliminary discussion on three parameters, Open Dermatol. J. 4 (110-115) (2010) 57.
[212] M. Elgamal, Automatic skin cancer images classification, IJACSA) Int. J. Adv. Comput. Sci. Appl. 4 (3) (2013) 287–294.
[213] A. Sáez, B. Acha, C. Serrano, Pattern analysis in dermoscopic images, in: Computer Vision Techniques for the Diagnosis of Skin Cancer, Springer, Berlin, Heidelberg, 2014, http://dx.doi.org/10.1007/978-3-642-39608-3_2 (pp. 23–48).
[214] S.O. Skr, T.R. Schopf, K. Thon, M. Zortea, M. Geilhufe, H.M. Kirchesch, F. Godtliebsen, A computer aided diagnostic system for malignant melanomas, in: Applied Sciences in Biomedical and Communication Technologies (ISABEL), 2010 3rd International Symposium on, IEEE, 2010, pp. 1–5 (November).
[215] A.F.M. Hani, H. Fitriyah, E. Prakasa, V.S. Asirvadam, S.H. Hussein, M.A. Azura, In vivo 3D thickness measurement of skin lesion, in: IEEE Conference on Biomedical Engineering and Sciences, Kuala Lumpur,N Ovember 30-December 2, IEEE, 2010, pp. 155–160.
[216] Y. Lu, I. Cohen, X.S. Zhou, Q. Tian, Feature selection using principal feature analysis, Proc of the 15th ACM International Conference on Multimedia (2009) 301–304.
[217] T. Roß, H. Handels, J. Kreusch, H. Busche, H.H. Wolf, S.J. Pöppl, Automatic classification of skin tumours with high resolution surface profiles, in: V. Hlaváč, R. Šára (Eds.), Computer Analysis of Images and Patterns. CAIP 1995. Lecture Notes in Computer Science, vol. 970, Springer, Berlin, Heidelberg, 1995.
[218] Chien-Hsing Chou, Yi-Zeng Hsieh, Chi-Yi Tsai, Modified sequential floating search algorithm with a novel ranking method, Int. J. Innov. Comput. Inf. Control 8 (3) (2012) 2089–2100.
[219] P. Somol, P. Pudil, J. Novovicova, P. Paclık, Adaptive floating search methods in feature selection, Pattern Recognit. Lett. 20 (11) (1999) 1157–1163.
[220] D. Devakumari, K. Thangavel, Analysis of adaptive floating search feature selection algorithm, in: Computer Networks and Information Technologies, Springer, Berlin, Heidelberg, 2011, pp. 526–530.
[221] H. Ganster, P. Pinz, R. Rohrer, E. Wildling, M. Binder, H. Kittler, Automated melanoma recognition, IEEE Trans. Med. Imaging 20 (3) (2001) 233–239.
[222] K. Kira, L. Rendell, A practical approach to feature selection, Proc of the Ninth International Conference on Machine Learning (1992) 249–256.
[223] M. Robnik-Sikonja, I. Kononenko, Theoretical and empirical analysis of ReliefF and RReliefF, Mach. Learn. 53 (2003) 23–69.
[224] Roberto Battiti, Using mutual information for selecting features in supervised neural net learning, IEEE Trans. Neural Netw. 5 (4) (1994) 537–550.
[225] L. Yu, H. Liu, Feature selection for high-dimensional data: a fast correlation-based filter solution Icml, vol. 3, 2003, pp. 856–863, August (pp. 856–863).
[226] Luis Talavera, An evaluation of filter and wrapper methods for feature selection in categorical clustering, in: Advances in Intelligent Data Analysis VI, Springer, Berlin, Heidelberg, 2005, pp. 440–451.
[227] R.J. Friedman, D. Gutkowicz-Krusin, M.J. Farber, M. Warycha, L. Schneider-Kels, N. Papastathis, M.C. Mihm, P. Googe, R. King, V.G. Prieto, A.W. Kopf, The diagnostic performance of expert dermoscopists vs a computer-vision system on small-diameter melanomas, Arch. Dermatol. 144 (4) (2008) 476–482.
[228] N. Sanchez-Marono, A. Alonso-Betanzos, M. Tombilla-Sanroman, Filter methods for feature selection?a comparative study, in: Intelligent Data Engineering and Automated Learning-IDEAL, Springer, Berlin, Heidelberg, 2007, pp. 178–187.
[229] L.K. Ferris, R.J. Harris, New diagnostic aids for melanoma, Dermatol. Clin. 30 (3) (2012) 5.
[230] Ron Kohavi, George H. John, Wrappers for feature subset selection, Artif. Intell. 97 (1) (1997) 273–324.
[231] I. Guyon, J. Weston, S. Barnhill, V. Vapnik, Gene selection for cancer classification using support vector machines, Mach. Learn. 46 (1–3) (2002) 389–422.
[232] Paulo Eduardo Rauber, R.R.O.D. Silva, Sander Feringa, M. Emre Celebi, A.X. Falao, Alexandru C. Telea, Interactive image feature selection aided by dimensionality reduction, EuroVis Workshop on Visual Analytics (EuroVA). The Eurographics Association (2015).
[233] Mutlu Mete, Nikolay Metodiev Sirakov, Optimal set of features for accurate skin cancer diagnosis, Proc 2014 IEEE International Conference On. Image Processing (ICIP) (2014) 2256–2260.
[234] E. Fix, J.L. Hodges Jr., Discriminatory Analysis-nonparametric Discrimination: Consistency Properties, California Univ Berkeley, 1951, http://dx.doi.org/10.1037/e471672008-001.
[235] Kiran Ramlakhan, Yi Shang, A mobile automated skin lesion classification system, Proc 23rd IEEE International Conference on Tools with Artificial Intelligence (ICTAI) (2011) 138–141.
[236] M. Otzeta, B. Sierra, E. Lazkano, A. Astigarraga, Classifier hierarchy learning by means of genetic algorithms, Pattern Recognit. Lett. 27 (16) (2006) 1998–2004.
[237] A.K. Jain, R.P.W. Duin, J. Mao, Statistical pattern recognition: a review, IEEE Trans. Pattern Anal. Mach. Intell. 22 (1) (2000) 4–37.
[238] Eva Armengol, Classification of melanomas in situ using knowledge discovery with explained case-based reasoning, Artif. Intell. Med. 51 (2) (2011) 93–105.
[239] I. Giotis, N. Molders, S. Land, M. Biehl, M.F. Jonkman, N. Petkov, MED-NODE: a computer-assisted melanoma diagnosis system using non-dermoscopic images, Expert. Syst. Appl. 42 (19) (2015) 6578–6585.
[240] M. Law, A Simple Introduction to Support Vector Machines. Lecture for CSE, 802, 2006.
[241] Jozsef Valyon, Gabor Horvath, A weighted generalized LS-SVM, Periodica Polytechnica, Electrical Eng. 47 (3) (2003) 229–251.
[242] V. Vapnik, Statistical Learning Theory, Wiley, New York, 1998, pp. 1998.
[243] F. Ercal, A. Chawla, W.V. Stoecker, H.C. Lee, R.H. Moss, Neural network diagnosis of malignant melanoma from color images, IEEE Trans. Biomed. Eng. 41 (9) (1994) 837–845.

[244] Ilias Maglogiannis, Elias Zafiropoulos, Christos Kyranoudis, Intelligent segmentation and classification of pigmented skin lesions in dermatological images, in: Advances in Artificial Intelligence, Springer, Berlin, Heidelberg, 2006, pp. 214–223.
[245] E.L. Torre, B. Caputo, T. Tommasi, Melanoma Recognition Using Kernel Classifiers (No. LIDIAP-REPORT-2006-012), IDIAP, 2006.
[246] K. Grzesiak-Kopeć, L. Nowak, M. Ogorzałek, Automatic diagnosis of melanoid skin lesions using machine learning methods, in: International Conference on Artificial Intelligence and Soft Computing, Springer International Publishing, 2015, pp. 577–585 (June);
Y. Shen, Loss functions for binary classification and class probability estimation, in: Doctoral dissertation, University of Pennsylvania, 2005.
[247] Q. Abbas, M. Sadaf, A. Akram, Prediction of dermoscopy patterns for recognition of both melanocytic and non-Melanocytic skin lesions, Computers 5 (3) (2016) 13.
[248] Maglogiannis Ilias, Sotiris Pavlopoulos, Dimitrios Koutsouris, An integrated computer supported acquisition, handling, and characterization system for pigmented skin lesions in dermatological images, IEEE Trans. Inf. Technol. Biomed. 9 (1) (2005) 86–98.
[249] M. Welling, Fisher Linear Discriminant Analysis, 3, Department of Computer Science, University of Toronto, 2005, pp. 1–4.
[250] S. Greenland, The need for reorientation toward cost-effective prediction, Stat. Med. 27 (2008) 199–206.
[251] D. Piccolo, A. Ferrari, K. Peris, R. Diadone, B. Ruggeri, S. Chimenti, Dermoscopic diagnosis by a trained clinician vs. a clinician with minimal dermoscopy training vs. computer-aided diagnosis of 341 pigmented skin lesions: a comparative study, Br. J. Dermatol. 147 (3) (2002) 481–486.
[252] M. Binder, H. Kittler, A. Seeber, A. Steiner, H. Pehamberger, K. Wolff, Epiluminescence microscopy-based classification of pigmented skin lesions using computerized image analysis and an artificial neural network, Melanoma Res. 8 (3) (1998) 261–266.
[253] A. Mehta, A.S. Parihar, N. Mehta, Supervised classification of dermoscopic images using optimized fuzzy clustering based Multi-Layer Feed-forward Neural Network, in: Computer, Communication and Control (IC4), 2015 International Conference on, IEEE, 2015, pp. 1–6 (September).
[254] K. Przystalski, L. Nowak, M. Ogorzalek, G. Surowka, Semantic analysis of skin lesions using radial basis function neural networks, Proc Human System Interactions (HSI) IEEE Conference (2010) 128–132.
[255] B. Burke Harry, Artificial neural networks for cancer research: outcome prediction, Semin. Surg. Oncol. 10 (1) (1994) (John Wiley & Sons Inc.).
[256] S. Dreiseitl, L. Ohno-Machado, H. Kittler, S. Vinterbo, H. Billhardt, M. Binder, A comparison of machine learning methods for the diagnosis of pigmented skin lesions, J. Biomed. Inform. 34 (1) (2001) 28–36.
[257] G. Litjens, T. Kooi, B.E. Bejnordi, A.A.A. Setio, F. Ciompi, M. Ghafoorian, et al., A Survey on Deep Learning in Medical Image Analysis, 2017 (arXiv preprint arXiv:1702.05747).
[258] N. Codella, J. Cai, M. Abedini, R. Garnavi, A. Halpern, J.R. Smith, Deep learning, sparse coding, and SVM for melanoma recognition in dermoscopy images, in: International Workshop on Machine Learning in Medical Imaging, Springer International Publishing, 2015, October (pp. 118–126).
[259] J. Kawahara, A. BenTaieb, G. Hamarneh, Deep features to classify skin lesions, Proc. IEEE 13th Int. Symp. Biomed. Imag. (ISBI), Aug. (2016).
[260] A.J. Vickers, E.B. Elkin, Decision curve analysis: a novel method for evaluating prediction models, Med. Decis. Making 26 (2006) 565–574.
[261] S. Ioffe, C. Szegedy, Batch Normalization: Accelerating Deep Network Training by Reducing Internal Covariate Shift, 2015 (arXiv preprint arXiv:1502.03167).
[262] K. He, X. Zhang, S. Ren, J. Sun, Deep residual learning for image recognition, Proceedings of the IEEE Conference on Computer Vision and Pattern Recognition (2016) (pp. 770–778).
[263] E. Nasr-Esfahani, S. Samavi, N. Karimi, S.M.R. Soroushmehr, M.H. Jafari, K. Ward, K. Najarian, Melanoma detection by analysis of clinical images using convolutional neural network, in: Engineering in Medicine and Biology Society (EMBC), 2016 IEEE 38th Annual International Conference of the, IEEE, 2016, pp. 1373–1376 (August).
[264] T. Yoshida, M.E. Celebi, G. Schaefer, H. Iyatomi, Simple and effective pre-processing for automated melanoma discrimination based on cytological findings, Big Data (Big Data), 2016 IEEE International Conference on (2016) 3439–3442 (December).
[265] K. Matsunaga, A. Hamada, A. Minagawa, H. Koga, Image Classification of Melanoma, Nevus and Seborrheic Keratosis by Deep Neural Network Ensemble, 2017 (arXiv preprint arXiv:1703.03108.).
[266] M. Zorman, M.M. Stiglic, K. Peter, I. Maltic, The limitations of decision trees and automatic learning in real world medical decision making, J. Med. Syst. 21 (6) (1997) 403–415.
[267] Yu Zhou, Zhuoyi Song, Binary Decision Trees for Melanoma Diagnosis Multiple Classifier Systems, Springer, Berlin, Heidelberg, 2013, pp. 374–385.
[268] Wei-Yin Loh, Classification and regression trees, Wiley Interdiscip. Rev.: Data Mining Knowl. Discov. 1 (1) (2011) 14–23.
[269] M. Wiltgen, A. Gerger, J. Smolle, Tissue counter analysis of benign common nevi and malignant melanoma, Int. J. Med. Inf. 69 (2003) 17–28.
[270] Stephan Dreiseitl, Lucila Ohno-Machado, Logistic regression and artificial neural network classification models: a methodology review, J. Biomed. Inform. 35 (5) (2002) 352–359.
[271] Jonathan Kantor, Deborah E. Kantor, Routine dermatologist-performed full-body skin examination and early melanoma detection, Arch. Dermatol. 145 (8) (2009) 873–876.
[272] P.A. Gutierrez, C. Hervas-Martınez, Classification of melanoma presence and thickness based on computational image analysis Hybrid Artificial Intelligent Systems: 11th International Conference, HAIS 2016, Seville, Spain, April 18–20, 2016, Proceedings, vol. 9648, Springer, 2016 (May p. 427).
[273] G. Schaefer, B. Krawczyk, M.E. Celebi, H. Iyatomi, An ensemble classification approach for melanoma diagnosis, Memet Comput 6 (4) (2014) 233–240.
[274] M. Sadeghi, T.K. Lee, D. McLean, H. Lui, M.S. Atkins, Detection and analysis of irregular streaks in dermoscopic images of skin lesions, IEEE Trans. Med. Imaging 32 (5) (2013) 849–861.
[275] G. Capdehourat, A. Corez, A. Bazzano, R. Alonso, P. Musé, Toward a combined tool to assist dermatologists in melanoma detection from dermoscopic images of pigmented skin lesions, Pattern Recognit. Lett. 32 (16) (2011) 2187–2196.
[277] C.S. Silva, A.R. Marcal, Colour-based dermoscopy classi- fication of cutaneous lesions: an alternative approach, Comput. Methods Biomech. Biomed. Eng. Imag. Vis. 1 (4) (2013) 211–224.
[276] J. Premaladha, K.S. Ravichandran, Novel approaches for diagnosing melanoma skin lesions through supervised and deep learning algorithms, J. Med. Syst. 40 (4) (2016) 1–12.
[278] F. Xie, H. Fan, Y. Li, Z. Jiang, R. Meng, A. Bovik, Melanoma classification on dermoscopy images using a neural network ensemble model, IEEE Trans. Med. Imaging 36 (3) (2017) 849–858.
[279] Q. Abbas, Computer-aided decision support system for classification of pigmented skin lesions, Int. J. Comput. Sci. Network Security (IJCSNS) 16 (4) (2016) 9.
[280] Advances in Soft Computing: Engineering Design and Manufacturing, in: R. Roy, T. Furuhashi, P.K. Chawdhry (Eds.), Springer Science & Business Media, 2012.
[281] K. Shimizu, H. Iyatomi, M.E. Celebi, K.A. Norton, M. Tanaka, Four-class classification of skin lesions with task decomposition strategy, IEEE Trans. Biomed. Eng. 62 (1) (2015) 274–283.
[282] V. Berenguer, D. Ruiz, A. Soriano, Application of hidden markov models to melanoma diagnosis, in: International Symposium on Distributed Computing and Artificial Intelligence 2008 (DCAI 2008), Springer, Berlin/Heidelberg, 2009, pp. 357–365.
[283] A. Tenenhaus, A. Nkengne, J.F. Horn, C. Serruys, A. Giron, B. Fertil, Detection of melanoma from dermoscopic images of naevi acquired under uncontrolled conditions, Skin Res. Technol. 16 (1) (2010) 85–97.
[284] T. Chang, C.C. Kuo, Texture analysis and classification with tree-structured wavelet transform, IEEE Trans. Image Process. 2 (4) (1993) 429–441.
[285] S.V. Patwardhan, A.P. Dhawan, P.A. Relue, Classification of melanoma using tree structured wavelet transforms, Comput. Methods Programs Biomed. 72 (3) (2003) 223–239.
[286] S.V. Patwardhan, S. Dai, A.P. Dhawan, Multi-spectral image analysis and classification of melanoma using fuzzy membership based partitions, Comput. Med. Imaging Graph. 29 (4) (2005) 287–296.
[287] B. Salah, M. Alshraideh, R. Beidas, F. Hayajneh, Skin cancer recognition by using a neuro-fuzzy system, Cancer Inf. 10 (2011) 1.
[288] R. Kohavi, A study of cross-validation and bootstrap for accuracy estimation and model selection, IJCAI 14 (2) (1995) 1137–1145.
[289] J.-S.R. Jang, Self-learning fuzzy controllers based on temporal backpropagation, IEEE Trans. Neural Netw. 3 (5) (1992) 714–723.
[290] S.M. Odeh, Using an adaptive neuro-fuzzy inference system (AnFis) algorithm for automatic diagnosis of skin cancer, J. Commun. Comput. 8 (9) (2011) 751–755.
[291] E.W. Steyerberg, A.J. Vickers, N.R. Cook, T. Gerds, M. Gonen, N. Obuchowski, M.J. Pencina, M.W. Kattan, Assessing the performance of prediction models: a framework for traditional and novel measures, Epidemiology 21 (1) (2010) 128–138.
[292] S.K. Tasoulis, C.N. Doukas, I. Maglogiannis, V.P. Plagianakos, Classification of dermatological images using advanced clustering techniques, in: Annual International Conference of the IEEE, Engineering in Medicine and Biology Society (EMBC), 2010, pp. 6721–6724 (August).
[293] G.-B. Huang, H. Zhou, X. Ding, R. Zhang, Extreme learning machine for regression and multiclass classification, IEEE Trans. Syst. Man, Cybern. B, Cybern. 42 (April (2)) (2012) 513–529.
[294] J. Tang, C. Deng, G.B. Huang, Extreme learning machine for multilayer perceptron, IEEE Trans. Neural Networks Learn. Syst. 27 (4) (2016) 809–821.
[295] Suhail M. Odeh, Abdel Karim Mohamed Baareh, A comparison of classification methods as diagnostic system: a case study on skin lesions, Comput. Methods Programs Biomed. (2016), http://dx.doi.org/10.1016/j.cmpb.2016.09.012.

Sameena Pat**han** is currently pursuing PhD at MIT, Manipal. Her research interest includes Image Processing. She has more than 1 year of teaching and research experience. She has many publications in reputed national/international journals and conferences. She is a reviewer of journals published by Springer.

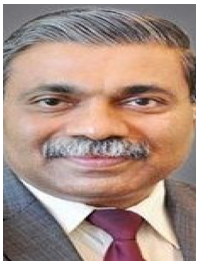

Dr. Gopalakrishna Prabhu acquired his B.E degree in Electronics & Communication Engineering from BIET, Davangere, Mysore University (1989), M.Tech degree in Biomedical Engineering MIT, Manipal with first rank from Mangalore University (1994) and PhD from IIT, Madras (2001). He is presently Professor in Biomedical Engineering and Director of Manipal Institute of technology, Manipal University, India. He has also served various managerial positions. His research area includes diagnostic imaging modalities and computer aided diagnosis.

Dr. P C Siddalingaswamy received his B.E degree in Electronics & communication Engineering from Kuvempu University (2000), M.Tech (2003) and PhD (2011) in Computer science from Manipal University, India. He is presently working as Associate Professor in Computer Science and Engineering at Manipal University. His research interests include medical image analysis and detection of visual abnormalities.